

# PeptideScience

THE AMERICAN PEPTIDE SOCIETY JOURNAL

## Special Issue: Materials and Applications

Guest Editor: Jean Chmielewski (Purdue University)

### EDITORIAL

Emerging designs and applications of peptide-based materials

Jean Chmielewski, *Peptide Science* 2021, doi: [10.1002/pep2.24226](https://doi.org/10.1002/pep2.24226)

### REVIEWS

A comparison of the collagen triple helix and coiled-coil peptide building blocks on metal ion-mediated supramolecular assembly

Ryan W. Curtis and Jean Chmielewski, *Peptide Science* 2021, doi: [10.1002/pep2.24190](https://doi.org/10.1002/pep2.24190)

Fluorinated peptide biomaterials

Janna N. Sloand, Michael A. Miller and Scott H. Medina, *Peptide Science* 2021, doi:

[10.1002/pep2.24184](https://doi.org/10.1002/pep2.24184)

Multivalent display of chemical signals on self-assembled peptide scaffolds

Hannah E. Distaffen, Christopher W. Jones, Brittany L. Abraham and Bradley L. Nilsson, *Peptide Science* 2021, doi:

[10.1002/pep2.24224](https://doi.org/10.1002/pep2.24224)

Peptides as key components in the design of non-viral vectors for gene delivery

Joseph Thomas, Kamia Punia and Jin Kim Montclare, *Peptide Science* 2021, doi: [10.1002/pep2.24189](https://doi.org/10.1002/pep2.24189)

Cyclic dipeptides: Biological activities and self-assembled materials

Kaili Zhao, Ruirui Xing and Xuehai Yan, *Peptide Science* 2021, doi: [10.1002/pep2.24202](https://doi.org/10.1002/pep2.24202)

Dual-peptide functionalized nanoparticles for therapeutic use

Chelsea R. Forest, Caitlin A. C. Silva and Pall Thordarson, *Peptide Science* 2021, doi: [10.1002/pep2.24205](https://doi.org/10.1002/pep2.24205)

Capturing nested information from disordered peptide phases

Christella K. Gordon, Regina Luu and David Lynn, *Peptide Science* 2021, doi: [10.1002/pep2.24215](https://doi.org/10.1002/pep2.24215)

### ARTICLES

Enzymatically forming cell compatible supramolecular assemblies of tryptophan-rich short peptides

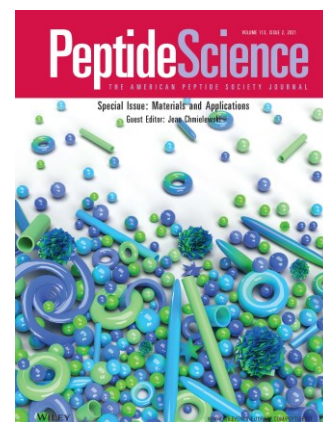
Dongsik Yang, Beom Jin Kim, Hongjian He and Bing Xu, *Peptide Science* 2021, doi: [10.1002/pep2.24173](https://doi.org/10.1002/pep2.24173)

Short self-assembling peptides with a urea bond: A new type of supramolecular peptide hydrogel materials

Hiroshi Tsutsumi, Kunifumi Tanaka, Jyh Yea Chia and Hisakazu Mihara, *Peptide Science* 2021, doi: [10.1002/pep2.24214](https://doi.org/10.1002/pep2.24214)

Functionalized peptide hydrogels as tunable extracellular matrix mimics for biological applications

Katharina S. Hellmund, Benjamin von Lospichl, Christoph Böttcher, Kai Ludwig, Uwe Keiderling, Laurence Noirez, Annika Weiß, Dorian J. Mikolajczak, Michael Gradzielski and Beate Koks, *Peptide Science* 2021, doi: [10.1002/pep2.24201](https://doi.org/10.1002/pep2.24201)



# PeptideScience

THE AMERICAN PEPTIDE SOCIETY JOURNAL

## Special Issue: Materials and Applications

Guest Editor: Jean Chmielewski (Purdue University)

Piezoelectric properties reflecting nanostructures of tetrathiafulvalene and chloranil complexes using cyclic peptide nanotube scaffolds

Hiroshi Ohmura, Yuki Tabata, Shunsaku Kimura and Hirotaka Uji, *Peptide Science* 2021, doi: [10.1002/pep2.24192](https://doi.org/10.1002/pep2.24192)

Effect of side chain phenyl group on the self-assembled morphology of dipeptide hydrazides

Taku Ohtomi, Sayuri L Higashi, Daisuke Mori, Aya Shibata, Yoshiaki Kitamura and Masato Ikeda, *Peptide Science* 2021, doi: [10.1002/pep2.24200](https://doi.org/10.1002/pep2.24200)

Self-assembling cyclic peptide-oligonucleotide conjugates: Synthetic strategies and the effect of cyclic topology on self-assembly and base pairing

Mahnseok Kye, Zhihao Zhang and Yong-beom Lim, *Peptide Science* 2021, doi: [10.1002/pep2.24193](https://doi.org/10.1002/pep2.24193)

Modifying the surface of peptide nanofibers utilizing a thiol-thioester exchange

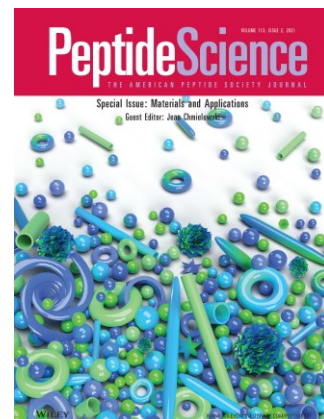
Ramiz Haddad, Elizabeth Ferraro, Ashley Halmans and Jillian E. Smith-Carpenter, *Peptide Science* 2021, doi: [10.1002/pep2.24169](https://doi.org/10.1002/pep2.24169)

Nanostructures from protected L/L and D/L amino acid containing dipeptides

Rajat Subhra Giri, Saikat Pal, Sayanta Roy, Gobinda Dolai, Srinivasa Rao Manne, Sandip Paul and Bhubaneswar Mandal, *Peptide Science* 2021, doi: [10.1002/pep2.24176](https://doi.org/10.1002/pep2.24176)

Self-assembly of hairpin peptides mediated by Cu(II) ion: Effect of amino acid sequence

Jiqian Wang, Chengdong Wang, Yanqing Ge, Yawei Sun, Dong Wang, and Hai Xu, *Peptide Science* 2021, doi: [10.1002/pep2.24208](https://doi.org/10.1002/pep2.24208)



**REVIEW**

# Peptides as key components in the design of non-viral vectors for gene delivery

Joseph Thomas<sup>1,2</sup> | Kamia Punia<sup>1</sup> | Jin Kim Montclare<sup>1,2,3,4</sup> 

<sup>1</sup>Department of Chemical and Biomolecular Engineering, New York University Tandon School of Engineering, Brooklyn, New York, USA

<sup>2</sup>Department of Biochemistry, SUNY Downstate Medical Center, Brooklyn, New York, USA

<sup>3</sup>Department of Chemistry, New York University, New York, New York, USA

<sup>4</sup>Department of Biomaterials, New York University College of Dentistry, New York, New York, USA

**Correspondence**

Jin Kim Montclare, Department of Biochemistry, SUNY Downstate Medical Center, Brooklyn, NY 11203, USA.  
Email: montclare@nyu.edu

**Funding information**

Army Research Office, Grant/Award Numbers: W911NF-19-1-0150, W911NF-19-2-0160; Division of Materials Research, Grant/Award Numbers: DMR 1505214, DMR 1728858; National Center for Advancing Translational Sciences, Grant/Award Number: UL1 TR000038; National Center for Advancing Translational Sciences, National Institutes of Health, Grant/Award Number: UL1 TR000038; NYU Shiffrin-Myers Breast Cancer Discovery Fund

**Abstract**

Successful clinical implementation of gene delivery relies on the use of viral or non-viral based vectors to package and protect the therapeutic nucleic acid. These vehicles must also be able to direct the fate of the cargo once it has entered the cell to ensure that the nucleic acid is functional, and the desired outcome is achieved. Compared to viral vectors, non-viral vectors have the advantage of incorporating different material types such as lipids, polymers, and peptides to tune overall safety and efficacy. Peptides are especially powerful when used in gene delivery vectors as they are able to increase gene delivery efficacy by introducing new biochemical functionality. This review will discuss the use of peptides as central design components in non-viral gene delivery vectors. The contribution of the peptide component to the overall functionality of the delivery vehicle will be highlighted, with a focus on peptides as the only vehicle component or peptides in complex assemblies with lipids or polymers.

**KEYWORDS**

biomaterials, gene delivery, peptide, polypeptide, nucleic acid

## 1 | INTRODUCTION

Nucleic acids possess critical instructions for controlling biological function, and as a new class of therapeutic agent have the potential to make a broad impact in biotechnology and medicine.<sup>[1]</sup> There is an urgent need for gene therapies to alleviate various pathological conditions but the ability to produce an effective vector that can deliver therapeutic genes still presents many technical challenges.<sup>[2–4]</sup> The intracellular delivery of nucleic acids presents a particularly difficult challenge, because the nucleic acid must cross the plasma membrane and be protected from nucleases. Once inside the cell, the nucleic acid must escape from the endosome and be released into the cytoplasm to perform its function.<sup>[5]</sup> All of these physical and biological barriers pose a significant engineering problem, and many vectors have been

created in an attempt to bring clinical gene therapy into reality. Efforts are underway to develop vehicles composed from modified viruses,<sup>[2,6]</sup> polymers,<sup>[7,8]</sup> lipids,<sup>[8–10]</sup> cell penetrating peptides,<sup>[11,12]</sup> and other nano-assemblies.<sup>[13–15]</sup> Virus based vectors can package nucleic acids and facilitate integration into the genome of the transfected cell resulting in long term, stable expression.<sup>[2]</sup> These vectors can elicit a detrimental immune response, and so far, have mainly been explored for clinical use in tissues like the eye that are immunologically privileged.<sup>[16]</sup> Polymers have been explored since they offer the ability to create higher order structures based on the properties of tunable monomers, however they also suffer from the potential for high immunogenicity, as well as complicated synthetic reaction schemes that are needed to create homogenous particles.<sup>[8]</sup> Cationic lipids are viewed as a safer alternative to polymers, but recent

evidence has shown that these vectors can also provoke a harmful immune response at therapeutically relevant doses.<sup>[8,17]</sup>

Cell penetrating peptides (CPP) are a subset of peptides that can condense nucleic acids through electrostatic interactions and have been investigated as non-viral gene carriers since the 1980's.<sup>[36]</sup> CPPs are short chains of amino acids that assemble to form unique structures with distinct chemical properties. These chains can be synthesized via solid phase synthesis or recombinant methods, and provide the advantage of being tunable at the monomer level.<sup>[37]</sup> CPPs can also be combined with other materials such as polymers, lipids, and other more complex nano-assemblies to augment existing delivery properties.<sup>[12,31,38,39]</sup> The sequences of CPPs allow them to cross the cell membrane, but challenges such as serum stability and endosomal escape present hurdles to successful gene delivery.<sup>[8]</sup> The use of polyethylene glycol<sup>[40]</sup> and groups capable of disrupting the endosome to release intact cargo<sup>[33]</sup> are being explored to address these shortcomings, but more work must be done before peptide-based gene delivery vehicles reach high enough levels of efficacy to become clinically relevant.

In this review, advances in the use of specific peptide sequences (Table 1) for the delivery of nucleic acids will be covered in various non-viral vehicle formulations. Linear and branched peptide chains will be discussed as they are the most straight-forward use of specific sequences and much work is being done to optimize these materials as gene delivery vectors. Peptides that are conjugated to other materials or used in complex nanoparticle formulations will also be discussed, as these methods introduce higher

levels of functionality to the delivery vectors but still rely on the peptide sequence as a core functional component. Peptide materials that integrate polymer, lipid, and stimuli responsive components to optimize gene delivery are also discussed in order to demonstrate the versatility of CPP's in various delivery systems. The examination of a wide range of peptide-based materials provides a high level view of where design methodologies incorporating peptides as central functional component fit into the non-viral gene delivery landscape, and allows for a forward look into the application of new design strategies on the horizon that have the potential to bring safe gene therapy into widespread clinical use.

## 2 | PEPTIDES FOR GENE DELIVERY

CPPs are biocompatible and can be synthesized using a variety of well understood techniques,<sup>[41,42]</sup> making them an attractive alternative to synthetic polymers. The ability to tune the sequence at the amino acid level provides a wide arena for material exploration, and many different types of cationic peptides have been identified that can condense nucleic acids, penetrate the cell membrane, and release functional cargo to the cytoplasm or nucleus.<sup>[43]</sup> These materials range from simple repeats of a cationic amino acid, such as lysine or arginine, all the way to complex sequences derived from viral proteins.<sup>[44,45]</sup> In this section we will discuss specific examples of CPPs and their use as agents driving nucleic acid transfection.

Name	Peptide sequence	Function
rPOA	Cys-(D-R9)-Cys	Gene delivery <i>in vivo</i> <sup>[18]</sup>
Branched oligoarginine	Cys-R9-Cys-R9-Cys	Increased particle size and gene loading <sup>[19]</sup>
ε-PLL Poly-l-lysine SL-I <sub>15</sub> mPEG-SS-PLL	KKKKKKKKKKKKKKKKKKKKKKKK	Cationic, naturally occurring <sup>[20,21]</sup>
TAT mTat	GRKKRRQRRR CHHHHH-Tat-HHHHHC	Fusogenic, membrane disrupting <sup>[22,23]</sup>
BTAT	Cys-GRKKRRQRRR-Cys-GRKKRRQRRR-Cys	Branched, fusogenic <sup>[24]</sup>
R3V6	RRRVVVVVV	Micelle forming <sup>[25]</sup>
GE11	YHWYGYTPQNV	Bilayer forming <sup>[26]</sup>
Pepfect 14	stearyl-AGYLLGKLLLOOLAAAALLOOLL-NH <sub>2</sub>	Cationic, cell penetrating <sup>[27,28]</sup>
CSP.DNA.FG lipoproteplex	MRGSHHHHHHGSGRLRP QMLRELQRTNAALRDVRELL RQQV KEITRLKNTVRRSRASGKLN	Cationic <sup>[29]</sup>
DNC:CSP:siRNA lipoproteplex	MRGSHHHHHHGSGRL RPQMLRELQRTNAALRDVRELLRQQV KEITRLKNTVRRSRASGKLN	Cationic <sup>[30]</sup>
P-(R <sub>8</sub> ) <sub>8,6</sub> -(HA <sub>2</sub> ) <sub>7,6</sub> -FITC	HA <sub>2</sub> - GLFGAIAGFIENGWEGMIDGK R8-KRRRRRRRR	HA <sub>2</sub> - membrane disrupting R8-cell penetrating <sup>[31]</sup>
Penetratin-PAMAM	RQKIWFQNRMMKWK	Cell penetrating <sup>[32]</sup>
VIPER	GLGAVLKVLTGLPALISWIKRKRQQ	Fusogenic, membrane disrupting <sup>[33]</sup>
PPDDBP	CP <sub>5</sub> K	ROS responsive <sup>[34]</sup>
REDV-mPEG-b-PLGA-g-PEI	CREVVV	Targeting endothelial cells <sup>[35]</sup>

**TABLE 1** Peptide-based constructs for gene delivery

## 2.1 | Oligoarginine

Some of the first gene delivering peptides explored were repeats of amino acid like lysine or arginine.<sup>[36,46]</sup> Both lysine and arginine are cationic amino acids with the ability to complex with the negatively charged phosphodiester backbone of nucleic acids via electrostatic interactions. These peptides of varying chain lengths will form aggregates when bound to nucleic acids that can be internalized within the cell.<sup>[47]</sup> Previous work has shown that peptide-based vectors can be biocompatible and will not elicit a harmful immune response,<sup>[48,49]</sup> but at therapeutically relevant doses this benefit goes away. These materials are still being developed and continue to show promise as viable gene vectors for clinical use.

For example, Woo *et al.* published work in which they explored the biocompatibility of a modified oligoarginine for use in cardiac tissue.<sup>[18]</sup> This vector consisted of the Cys-(D-R9)-Cys repeat of reducible poly(oligo-D-arginine) (rPOA) to form an extended cationic chain. This peptide was able to condense and deliver DNA, RNA, and protein.<sup>[50]</sup> The group had shown previously that their vector was safe for use in lung and brain tissue,<sup>[51–53]</sup> but recognized that there was a need for a safe delivery vehicle to target cardiac disease. The group delivered a plasmid encoding for vascular endothelial growth factor (VEGF) to H9c2 rat cardiomyocytes as well as cardiac tissue in rat, as VEGF therapy has been shown to be an effective treatment for myocardial infarction.<sup>[54]</sup> H9c2 cells were transfected at a 1:2 weight ratio of rPOA/pDNA and viability of transfected cells was found to be 98.00%, determined by MTT assay. This was compared to a PEI/pDNA control which showed similar transfection efficiency to the rPOA complexes, but only showed a 50.78% viability. Transfection was assessed in a myocardial infarction rat model by detection of VEGF expression in ischemic cardiac tissue by immunohistochemistry. A PEI/pDNA control was utilized again, and the rPOA complexes resulted in a 2.5-fold higher expression of VEGF. Cell death in the ischemic region was measured after a week using TUNEL assay, and cell death was found to be lower in the rPOA/pDNA group vs the PEI/pDNA group. This work demonstrated the safety of the rPOA vector for use in-vivo in cardiac tissue, and was strengthened by previous work showing efficacy in other tissue types.<sup>[51–53]</sup>

The 3D architecture of oligoarginine for improved gene delivery efficacy is also being explored. Yoo and Lee *et al.* have designed a branched oligoarginine with reducible disulfide bonds at the branch points.<sup>[19]</sup> Previous reports showed that connecting cationic chains with cysteine residues increased molecular weight as well as delivery efficacy.<sup>[55]</sup> These disulfide bonds can be reduced by glutathione which is over-secreted in the cellular cytoplasm,<sup>[56]</sup> and will promote nucleic acid release into the cytoplasm. These peptide vectors are effective but still needs to be optimized by further modifications. Yoo and Lee *et al.* have hypothesized that creating a branched oligoarginine construct would increase nucleic acid loading, protection, and ultimately delivery to the cytoplasm. To accomplish this, cysteine residues are used as a linker between oligoarginine repeats, as well as at the ends of the sequence (Cys-R9-Cys-R9-Cys). This results in an oligoarginine scaffold with linking points on the ends and middle, which creates the branched structure known as B-mR9 (Figure 1).

Static light scattering is used to confirm the increased molecular weight due to branching, with a final molecular weight of 138 889 g/mol. Gel retardation assay shows that the branched B-m9 exhibits superior pDNA binding ability compared to linear oligoarginine and a PEI control. When incubated with DL-dithiothreitol (DTT), the disulfide linkages of B-mR9 are broken and pDNA binding is significantly impaired. Using a nitrogen to phosphorous (N/P) ratio of 15, transfection of plasmid in three different cells lines is assessed (HEK 293, HELA, and SKOV3) and compared to a PEI/pDNA control using flow cytometry. In all three cell lines, B-mR9 had a higher transfection efficiency than the PEI/pDNA control. Cell viability analysis reveals significant differences with the B-mR9/pDNA treatments yielding viabilities above 80% for all three cell lines, whereas the PEI/pDNA treatments yielded viabilities around 60%. This shows that the branched B-m9 peptide could deliver plasmid as the same rate as PEI, but it is able to do so much safer. Similar experiments have been performed to assess siRNA delivery for VEGF knockdown; at an N/P ratio of three the B-mR9 vector shows greater knockdown than PEI in all three cell lines. These results showcase the versatility of the peptide-based vector to be utilized as a smart material to deliver payloads safely and effectively.

## 2.2 | Polylysine

Polylysine materials have also been used with some success as gene delivery vectors.<sup>[57,58]</sup> Polylysine suffers from similar shortcomings as oligoarginine (i.e., low transfection efficiency) so ongoing strategies are being used to increase transfection efficiency while maintaining safety.  $\epsilon$ -Poly-L-lysine ( $\epsilon$ -PLL) is a cationic peptide that consists of a repeat of 25–35 lysine residues.<sup>[59]</sup> It is naturally produced by *Streptomyces albus* and *Lysinopolymerus* and is known to have antibacterial properties. Mandal *et al.* have explored this variant of  $\epsilon$ -PLL as a gene delivery vector with the potential to have higher transfection efficacy than commercially available 1000–5000 Da poly-L-lysine (PLL).<sup>[20]</sup> Transfection of a plasmid encoding eGFP has been carried out in multiple cell lines (MCF-7, HeLa, and HEK 293) using  $\epsilon$ -PLL, PLL, or SuperFect reagent as a control. The  $\epsilon$ -PLL exhibits a 3.5, 3.79, and 4.79-fold increase when compared to PLL in MCF-7, HeLa, and HEK 293 cells, respectively.  $\epsilon$ -PLL also outcompetes SuperFect reagent with a 1.60, 1.53, and 1.79-fold increase in MCF-7, HeLa, and HRK 293 cells, respectively although this effect was not statistically significant. Toxicity is assessed in all three cell lines, with  $\epsilon$ -PLL showing no toxicity, while PLL possesses roughly 20% toxicity in all cell lines.

3D assemblies of PLL are also being explored as alternatives to linear chains. For example, Walsh *et al.* have developed a star-shaped PLL varying the length of the peptide arms to see if they can successfully transfect mesenchymal stem cells (MSCs) for tissue engineering applications.<sup>[21]</sup> These star polymers consist of a variable amount of peptide arms surrounding a polypropyleneimine (PPI) dendrimer core (Figure 2). The polylysine arms are assembled to have 40 L-lysine repeats per arm via N-carboxyanhydride (NCA) ring opening polymerization. The number of total arms present on each particle is then varied to either 16, 32, or 64. The 64-star PLL demonstrate the highest number of cells transfected, with 24.6% of cells transfected at 7 days. At day 7, the 32-and

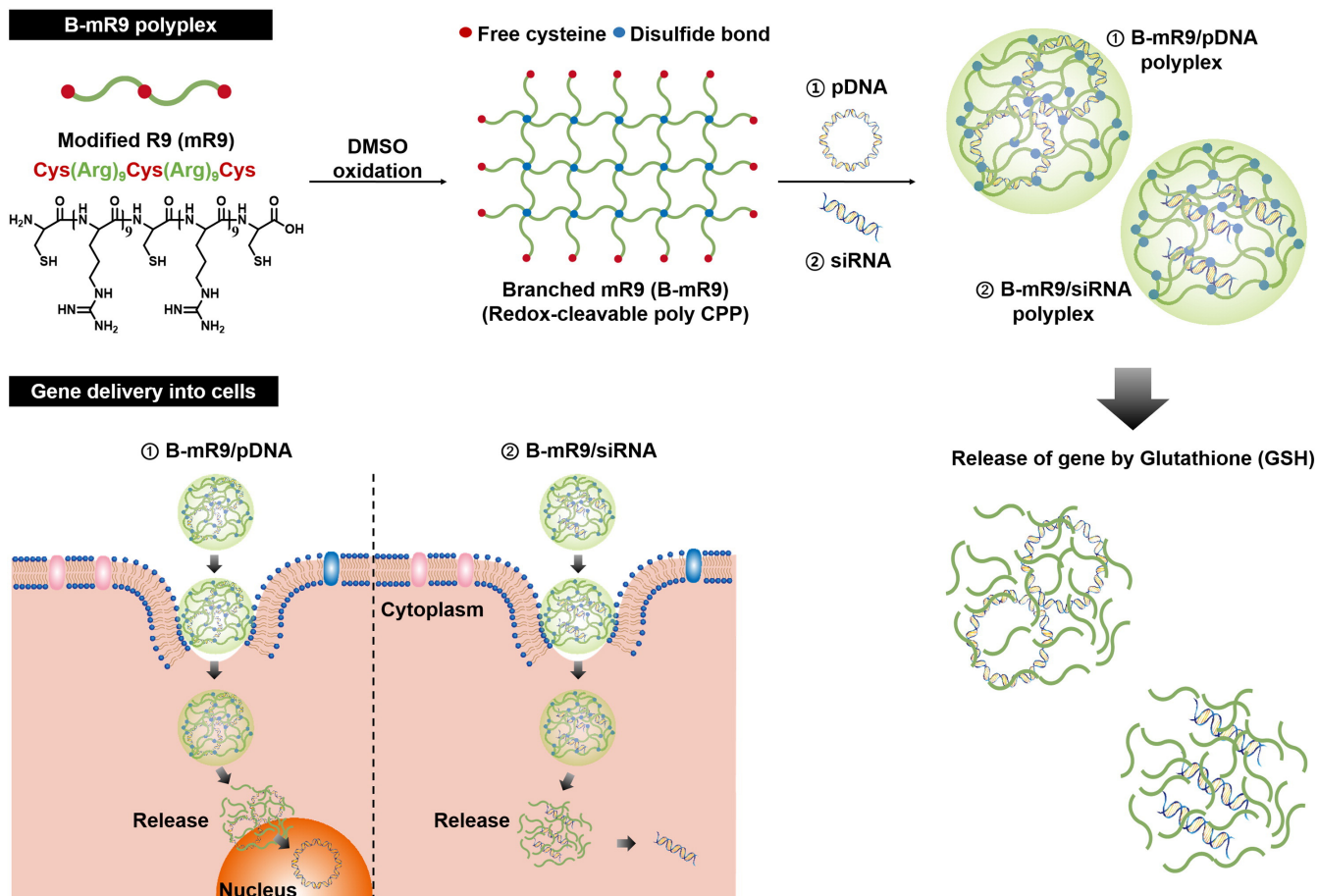


**FIGURE 1** Creating branched oligoarginine and mechanism of cellular transfection. Branched oligoarginine (B-mR9) is created by introduction of cysteine residues. Upon DMSO oxidation, a large branched network is formed. The positive charge of the arginine residues allows for complexation with pDNA or siRNA. The branched B-mR9/nucleic acid aggregate can then enter cells to release nucleic acid cargo through the action of glutathione. Reprinted with permission<sup>[19]</sup>

16-star PLLs transfect 22.3% and 2.0% of cells, respectively. Transfection efficiencies remain stable for all constructs until day 14 before declining. Linear PLL is only able to transfect 2.5% of cells at day 7, demonstrating that star PLLs with 32 or 64 peptide arms are able to transfect MSC's at a higher efficiency. PLL is an example of a simple peptide sequence being used in higher order assemblies that have much higher transfection efficiency than their linear counterparts. These types of materials allow for the expansion of agents that can be investigated for *in vivo* gene therapy, and also open up the opportunity that with low efficacy can be re-designed with new architecture.<sup>[60]</sup>

Cai *et al.* also explored the additions of polyethylene glycol (PEG) and imidazole to PLL to increase it *in vivo* circulation and vehicle endosomal escape.<sup>[61]</sup> The group previously described a PEGylated PLL that utilized a cysteine linker to release the PEG from the PLL in response to elevated glutathione levels, allowing for targeting of gene delivery to cancer cells.<sup>[40]</sup> This vehicle suffered from poor endosomal escape however, so imidazole groups were added via Schiff-base linkages to create a new PLL-based vehicle known as SL-I<sub>15</sub>mPEG-SS-PLL (Figure 3). This functionalization served two purposes: (a) the imidazole groups buffered endosomal pH and (b) the Schiff-base linkage could deprotonate at endosomal pH, promoting the loaded DNA

plasmid release. Gel retardation assay demonstrated that plasmid DNA was fully bound at weight/weight ratios higher than 0.15:1, and acid-base titration confirmed the buffering capacity of the imidazole groups. The release of PEG from the vehicle was confirmed via dynamic light scattering experiments. Stable particle sizes of  $181.0 \pm 6.2$  nm were observed. The addition of 10 mM glutathione cleaved the PEG groups and caused the cationic vehicle segments to aggregate, leading to increased particle size (>680 nm) after 4 hours. Transfection of MCF-7 cells with EGFP plasmid was assessed for SL-I<sub>15</sub>mPEG-SS-PLL, an optimized PEI-25k used as a positive control and mPEG-SS-PLL that did not contain the Schiff-base linked imidazole to isolate the improvements caused by the imidazole and Schiff-base groups (Figure 3). mPEG-SS-PLL successfully transfected 30% of cells while PEI-25k and SL-I<sub>15</sub>mPEG-SS-PLL transfected 40% of cells. Transfections were also carried out utilizing a luciferase plasmid with and without 20% serum. While a 13-fold decrease in luciferase transfection was observed for PEI-25 k after the addition of serum, SL-I<sub>15</sub>mPEG-SS-PLL did not see any significant decrease in transfection efficiency. This work demonstrated that shortcomings of peptide vectors, such as the inability of PLL to escape the endosome, could be remedied with clever engineering and modification.

**FIGURE 2** Schematic representing use of star-poly-L-lysine to transfect mesenchymal stem cells (MSCs). MSCs are hard to transfect, but star-shaped polylysine allows for effective condensation of pDNA that can cross the cell membrane *in vitro*. Reprinted with permission.<sup>[21]</sup> Copyright © 2018, American Chemical Society

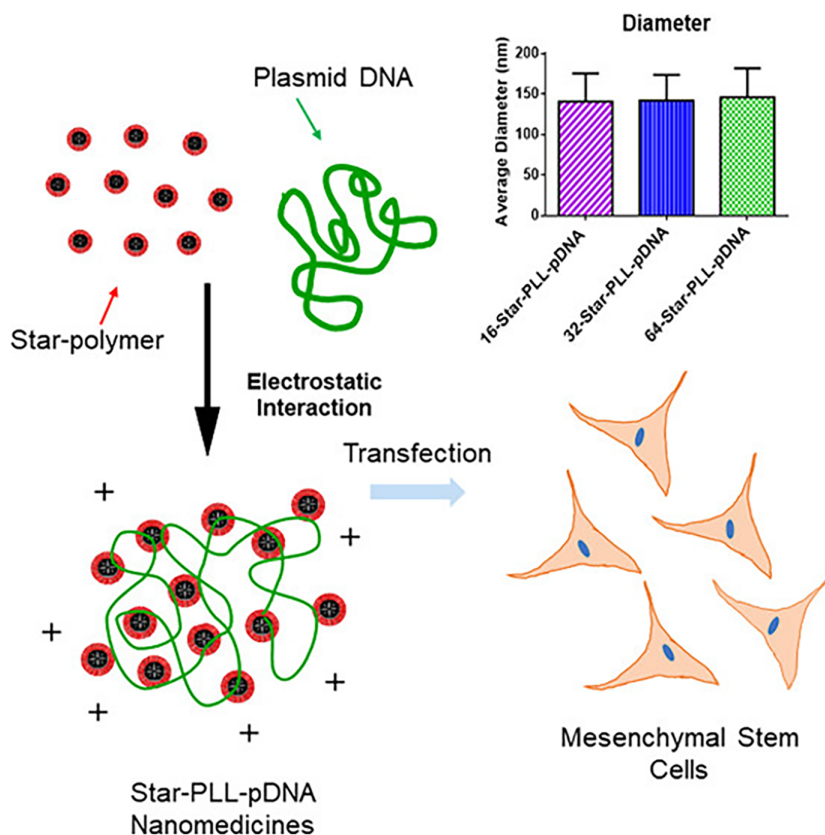
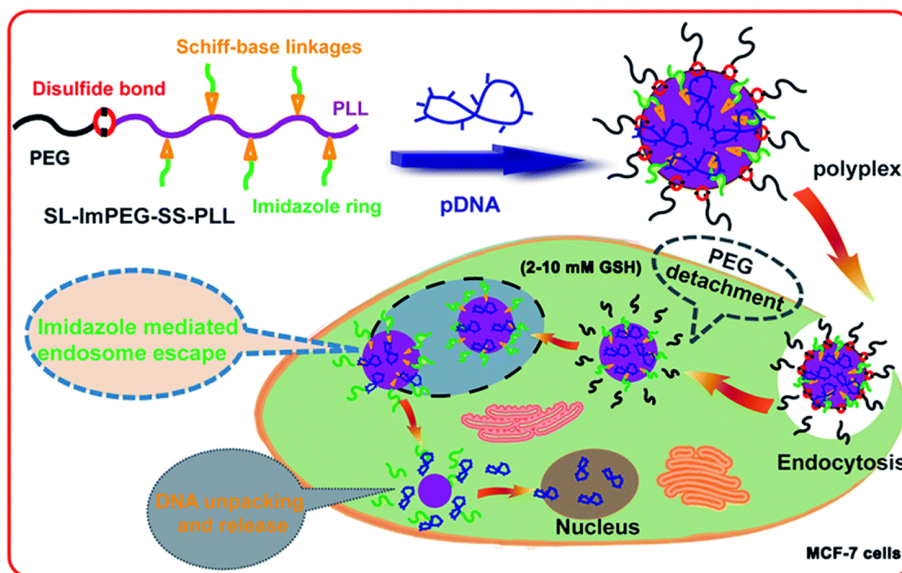


**FIGURE 3** PEG and imidazole modified PLL successfully transfects MCF-7 cells. The SL-ImPEG-SS-PLL vehicle can enter cancer cells and be de-PEGylated via high glutathione in the cytoplasm. Imidazole groups and Schiff-base linkages promote endosomal escape and plasmid DNA release respectively. Reprinted with permission<sup>[61]</sup>



### 2.3 | TAT

CPPs can also rely on structural disruption of membranes to gain entry into the cell.<sup>[44,62]</sup> CPPs can have the ability to change conformation once inside the cellular endosome, giving them properties of smart materials that can react to surrounding environmental conditions such as pH. These peptides can be derived from viruses or other sources and have been widely explored as gene delivery vectors due to their ability to condense nucleic acid and protect it from endosomal degradation.<sup>[45,63]</sup> The TAT peptide (GRKKRRQRRR) is a sequence

derived from an HIV protein transduction domain that imparts membrane disrupting behavior.<sup>[64,65]</sup> Modified versions of the TAT sequence, typically referred to as mTAT have been created in an effort to enhance cell penetrating and nucleic acid protection properties. Jeong *et al.* have created a modified TAT variant with interspersed and terminal cysteine residues in order to create a branched construct upon DMSO oxidation, known as BTAT.<sup>[24]</sup> Static light scattering experiments reveal that the molecular weight of the linear mTAT chain (3.4 kDa) increases to 294 kDa upon DMSO oxidation, and the clear liquid solution transitions to a clear gel indicating effective

disulfide bridge formation. Both linear TAT and mTAT as well as branched BTAT exhibits random coil structures, indicating that the disulfide linkages do not significantly affect secondary structure. The BTAT has a four-fold higher binding affinity to a plasmid coding for GFP than the linear TAT and mTAT, most likely due to the large branched network structure of BTAT. To determine if the branched construct outperforms the both the linear TAT and mTAT, flow cytometry analysis confirms BTAT having the highest transfection efficiency. Cell viability analysis illustrates that transfection with TAT, mTAT, or BTAT results in viability above 80% indicating safe transfection.

## 2.4 | Amphiphilic peptides

Amphiphilic peptides have also been explored for their nucleic acid delivery potential due to their ability to self-assemble into complex structures.<sup>[66,67]</sup> Song *et al.* have published analysis of a peptide called R3V6 for use as an antisense-oligodeoxynucleotide (antisense-ODN) delivery vehicle against miR-21 in glioblastoma.<sup>[25]</sup> miR-21 is a micro-RNA present in some cancers that is believed to have anti-apoptosis and pro-tumor survival activity.<sup>[68,69]</sup> R3V6 is a short peptide composed of three arginine repeats followed by six valine repeats. Previous work has shown that R3V6 has low delivery efficacy of pDNA *in vitro*, but could outcompete a 25 kDa PEI standard *in vivo* while showing lower toxicity.<sup>[70]</sup> In aqueous solution, R3V6 will spontaneously form micelles that have the ability to encapsulate hydrophobic drugs while still delivering nucleic acids.<sup>[71]</sup> Based on this, the authors have investigated the potential of using R3V6 to deliver antisense-ODN to rat glioblastoma cells (C6), to see if antisense-ODN/R3V6 particles have potential for use as an *in vivo* glioblastoma therapy. Gel retardation assay confirms that R3V6 can fully bind the antisense-ODN at a 2:1 weight ratio. Dynamic light scattering measurements show that when bound to the antisense-ODN, particles of  $135 \pm 21.8$  nm result with a zeta potential of  $15.8 \pm 0.77$  mV. Transfection of C6 cells is carried out through the use of a custom Renilla luciferase plasmid with an miR-21 recognition sequence present on the 5' untranslated region. This allows miR-21 that is present in the cells to bind to the plasmid and signal for its degradation through the RISC pathway.<sup>[25]</sup> If the antisense-ODN is successfully transfected however, it will bind to miR-21 and prevent it from destroying the plasmid. In this way, successful transfection can be reported through the luminescence of the expressed luciferase. Experiments reveal that antisense-ODN/R3V6 at a 1:30 weight ratio exhibits optimal transfection, with a 170% increase in luminescence signal compared to un-transfected control. Flow cytometry experiments are also performed through the use of a fluorescein (FAM) conjugated antisense-ODN. Results confirm that the R3V6 complexes delivers more antisense-ODN compared to the PEI 25k control. An MTT assay on C6 glioblastoma cells is used to determine if the R3V6 peptide could safely deliver the antisense-ODN. After treatment with the R3V6 complexes, an increase in cell death of 20% is observed after treatment compared to just below 60% for PEI 25k complexes. The delivery of a scrambled antisense-ODN results in minimal cell death compared to untreated controls for the

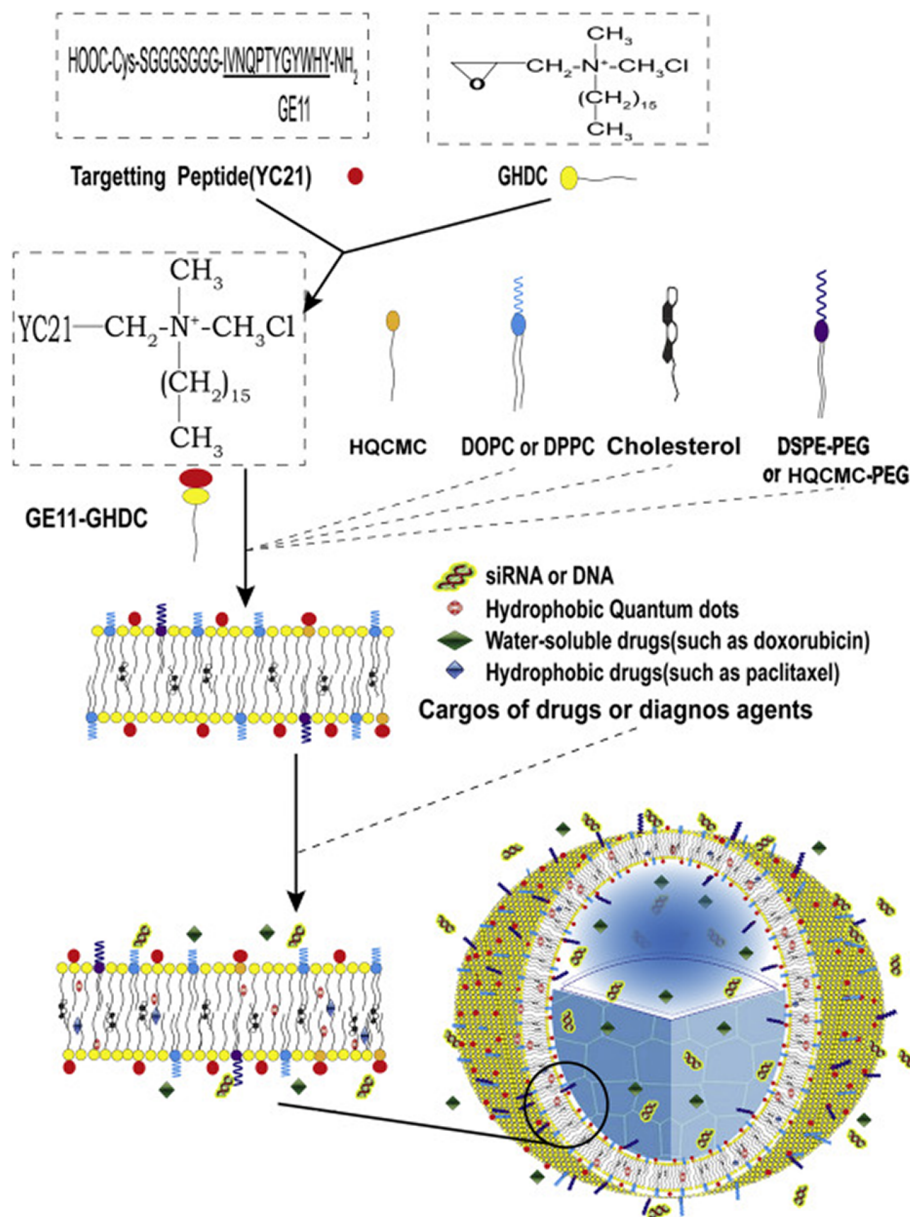
R3V6 complexes, while the PEI 25k complexes shows 60% viability. This demonstrates that the R3V6 peptide delivers antisense-ODN targeting miR-21 both more efficiently and more safely compared to PEI 25k, which is frequently used as a gold standard for non-viral gene delivery.<sup>[72-74]</sup>

Liang *et al.* have created a peptide amphiphile (PA) system that can self-assemble into bilayered nano-vesicles that can target epidermal growth factor receptors (EGFR) on the surface of EGFR positive cancer cells.<sup>[26]</sup> This is accomplished by using an 11 Amino acid stretch of an EGFR binding peptide known as GE11.<sup>[75-77]</sup> This peptide is conjugated to glycidyl hexadecyl dimethylammonium chloride (GHDC) in order to form the amphiphilic core of the bilayer nano-vesicle (Figure 4). Cholesterol was used to stabilize the bilayer to form the final vehicle known as ESPV. The resulting ESPV can also be further functionalized using other chemical agents in order to deliver hydrophobic drugs, quantum dots, or nucleic acids. For the case of pDNA and siRNA delivery, tetradecyl quaternised carboxymethyl chitosan (HQCMC) is added to provide a positive zeta potential for nucleic acid complexation. The resulting particles range from 10 to 400 nm with zeta potential ranging from 0 to 70 mV. UV-Vis spectroscopy confirms the presence of the GE11 peptide on the surface of the assembled ESPV, indicating that the sequence is available for recognition of EGFR on the cell surface. Gel retardation assay indicates that pDNA is fully bound at a weight ratio of 6:1 ESPV/pDNA. Three human cancer cell lines (SMMC-7721, Eca-109, and SGC-7901) have been transfected with a GFP plasmid in order to determine if the ESPV could target cells over-expressing EGFR. As a control, the ESPV minus the GE11 targeting peptide is also used. The two EGFP over-expressing lines (SMMC-7721 and Eca-109) shows higher fluorescence signal after transfection with peptide displaying ESPV compared to the vehicle without GE11. When SGC-7901 cells are transfected, no difference in fluorescence intensity is observed between the GE11 displaying ESPV and the ESPV minus GE11. This validates the design hypothesis that the GE11 peptide allows preferential transfection of EGFP over-expressing cells. Cytotoxicity assays of SMMC-7721 cells also reveals that the ESPV is not toxic to transfected cells. This work showcases how short peptide sequences can be used to form larger order structures that can be used to deliver nucleic acids to cells. The GE11 peptide is not considered a standard CPP, like other peptides discussed in this review, but it is still able to promote interactions with the target cell membrane to internalize nucleic acid cargo.

## 2.5 | Pepfect

Pepfects are a sub-family of CPP's that have been designed specifically for use in nucleic acid delivery.<sup>[78,79]</sup> Pepfects are able to transfect nucleic acid with a high efficiency and low cytotoxicity, with the added advantage of being able to transfect cells independent of their confluence. Pepfect 14 (PF14) is a particularly effective gene delivery agent that consists of a C-terminal stearyl moiety followed by a leucine and alanine heavy peptide chain (stearyl-AGYLLGKLLLO LAAAALLOOLL-NH<sub>2</sub>).<sup>[80]</sup> Ervin *et al.* have used PF14 as a way to safely

**FIGURE 4** Scheme of peptide amphiphile self-assembling into bilayer nano-vesicle with lipid components. The modular ESPV can be assembled with various components depending on its intended application. For siRNA delivery, the vehicle consists of GE11-GHDC, cholesterol, and HQCMC. Reprinted with permission<sup>[26]</sup>



transfect human embryonic stem cells (hES) in culture.<sup>[27]</sup> To probe the delivery of nucleic acid, an Alexa Fluor 568 conjugated siRNA is used to visualize transfection (Figure 5). Flow cytometry analysis 4 hours post-transfection reveals that 91% of cells are Alexa Fluor positive. Confocal microscopy confirmed that the fluorescence signal is from siRNA in the cytoplasm and not on the cell membrane. Live/dead cell counting is also performed to determine the cytotoxicity of the transfection complexes on the hES cells. At 20 nM siRNA concentration, the total number of living cells is not significantly different from untreated cells used as a control. This work demonstrates how CPP's can be used as a research tool to probe the function of proteins or genes through targeted nucleic acid delivery.

Urgard *et al.* have also explored the use of PF14 to transfect micro RNA (miRNA) into cultured cells.<sup>[28]</sup> They investigate the delivery of MiR-34a as a potential therapy for cancer, since MiR-34a has been shown to act as a tumor suppressor.<sup>[81,82]</sup> Previous work has been done to deliver micro RNA's using lipid reagents, but these

attempts have been largely unsuccessful due to low delivery efficiency and high toxicity.<sup>[83,84]</sup> Urgard *et al.* test the hypothesis that PF14 can transfect human primary prostate carcinoma-1 (PPC-1) cells more efficiently and safely compared to siPORT NeoFX, Lipofectamine 2000, and RNAiMAX. The PF14:MiR-34a complexes reveal sizes ranging from 100 to 1000 nm with negative surface charge when prepared at a 17:1 PF14:MiR-34a molar ratio. PPC-1 cells are transfected with these complexes and the amount of MiR-34a is measured using RT-PCR after 24 hours. Between a 1000-fold and 10 000-fold increase in MiR-34a levels are observed compared to un-transfected controls, verifying that PF14 can effectively deliver the microRNA to the cells. siPORT NeoFX is used as a positive control and shows similar levels of MiR-34a after transfection. A luminescent cell viability assay 48 hours after transfection revealed that only the PF14 safely delivers active MiR-34a to exert its tumor suppressive effects. This provides promising evidence that PF14 has potential as a safe nucleic acid delivery vector that warrants further exploration.

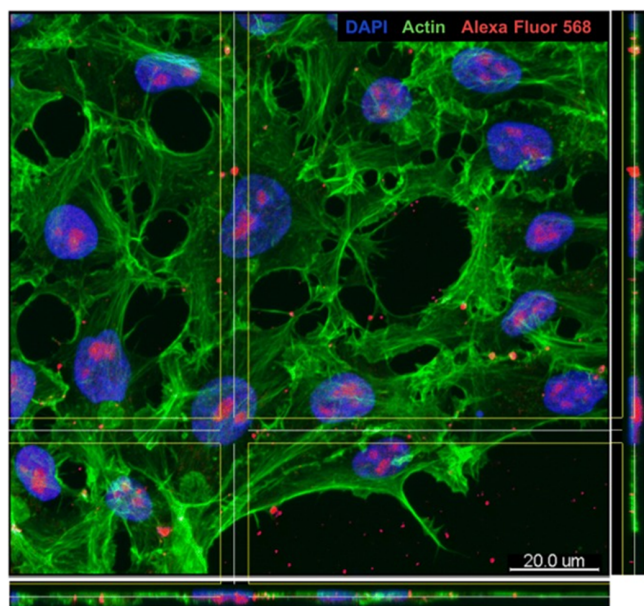


**FIGURE 5** Transfection of human embryonic stem cells using PF14:siRNA-Alexa Fluor. siRNA appears red, nucleus appears blue, and actin appears green. Pepfect 14 is able to deliver siRNA into hard to transfect cells. Content available through open source license<sup>[27]</sup>

### 3 | PEPTIDE-BASED LIPOPOLYPLEXES

Although there has been tremendous interest in CPPs due to their capability to efficiently condense nucleic acid, cationic peptide-based complexes can suffer from low transfection due to poor endosomal escape and lysosomal degradation.<sup>[85,86]</sup> Incorporation of various cationic lipids into polyplexes via non-covalent interactions to produce ternary complexes called lipopolyplexes (LPP) has been shown to considerably improve the transfection activity of CPPs.<sup>[87,88]</sup> Hence, extensive efforts are underway to investigate these cationic peptides/protein-based lipopolyplexes as gene delivery vehicles. Yamano *et al.* have developed a modified Tat peptide, known as mTat to deliver the gene for a  $\mu$ -opioid receptor (OPRM1) in ex vivo HSC-3 cells.<sup>[23]</sup> This Tat variant contains the Tat sequenced flanked by a cysteine and five histidine residues on each terminus. This construct is combined with commercially available FuGENE HD and used to transfect the HSC-3 cells prior to implantation in the paws of mice. RT-PCR assays confirms the expression of OPRM1 in the cells prior to implantation. Mice with transfected implants exhibit higher resilience to pain in their paw compared to HSC-3 implants transfected with GFP or implants that were not transfected at all, providing evidence that the transfected opioid receptor is functional. Cell proliferation assays at the tumor site confirm that there is no difference in cancer growth between transfected and non-transfected tumors. This data shows that the mTat:FuGENE HD lipopolyplex safely transfects a functional gene into cells.

Montclare and co-workers have engineered a coiled-coil supercharged protein (CSP) by mutating solvent exposed residues of the coiled-coil domain of cartilage oligomeric matrix protein (COMPcc) to positively charged arginine for effective condensation of nucleic acids.<sup>[29]</sup> To enhance gene delivery, CSP is further conjugated with the

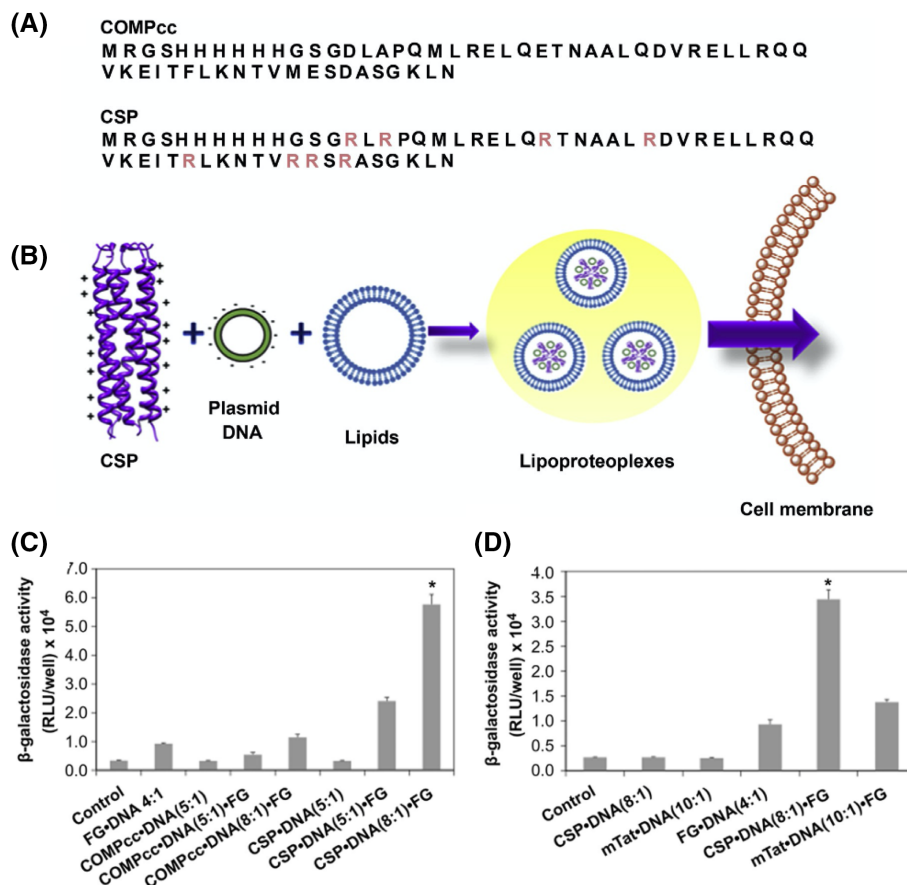
cationic lipid reagent Fugene (FG) via non-covalent interactions to generate the ternary complex called a “lipoproteoplex” (Figure 6B).  $\beta$ -Galactosidase plasmid DNA is incubated for 30 minutes with either CSP or COMPcc at various concentrations to form the proteoplexes. To determine the DNA binding ability of the proteins, electrophoretic mobility shift assay reveals that the supercharged CSP is highly proficient at condensing plasmid DNA, whereas COMPcc exhibits no binding ability. The proteoplexes are then mixed with FG at 4:1 wt./wt. ratio of lipid/DNA and incubated at room temperature for 15 minutes to generate lipoproteoplexes. *In vitro* transfection data indicates that the CSP lipoproteoplex significantly increases  $\beta$ -galactosidase activity in MC3T3-E1 mouse preosteoblasts compared to either FG or CSP alone (Figure 6C). Furthermore, the CSP lipoproteoplex also exhibit superior transfection efficiency as compared to previously designed mTat\*DNA\*FG lipopolyplexes (Figure 6D).

Rabbani *et al.* have engineered an LPP comprising a cationic lipid nanoparticle (CLN) composed of 1,2-dioleoyl-3-trimethylammonium-propane (DOTAP) and the edge activator sodium cholate (NaChol) to form DOTAP:NaChol (DNC) and CSP for topical siRNA delivery.<sup>[30]</sup> The DNC:CSP LPP demonstrated successful complexation of siRNA while producing non-cytotoxic and inherently flexible nanoparticles with diameter measuring  $160.94 \pm 34.21$  nm for 10:1:1 DNC:CSP:siRNA complex (LPP-10) as observed from the transmission electron microscopy (TEM) images. *In vitro* transfection efficacy of the LPP tested against GAPDH in 3T3 mouse fibroblasts confirmed high gene silencing with 62% mRNA knockdown for LPP-10. The *in vivo* efficacy of LPP is assessed in humanized murine diabetic wound healing model where wounds on mice were treated with LPP comprising siKeap1 which is a key repressor of a central regulator of antioxidant pathways called nuclear factor erythroid-2 like 2 (Nrf2). The diabetic mice treated with LPP-10 siKeap1 showed significantly enhanced diabetic wound healing which is similar to healing in wild type mice, with wound closure in  $22.25 \pm 1.97$  days for LPP-10 siKeap1 as compared to 31 days for LPP containing nonsense siRNA (siNS) LPP-10 siNS (Figure 7D). The ability of this novel LPP to efficiently encapsulate and topically deliver siRNA for diabetic wound healing demonstrates its effectiveness as a promising vehicle for non-viral gene delivery that can be translated into clinical use for treating diabetic patients with non-healing wounds.

### 4 | PEPTIDE-POLYMER HYBRIDS

Polymers comprised of positively charged moieties that are capable of condensing DNA into complexes known as polyplexes, have garnered significant attention in the field of gene therapy.<sup>[89,90]</sup> Decoration of bioactive peptides on these polymeric scaffolds generates physiologically stable complexes and enhances gene transfer efficacy by imparting multifunctional properties to the polyplexes. This can be done through bioactive peptides bearing fusogenic, stimuli responsive, or targeting moieties.<sup>[91–93]</sup> Peptide-polymer hybrids can be readily produced either by physical adsorption or by covalent conjugation techniques including post-polymer modifications<sup>[94]</sup> and polymerization of peptide conjugated monomers.<sup>[95]</sup> In this section we discuss different types of peptide-polymer hybrids for nucleic acid delivery.

**FIGURE 6** Supercharged protein-lipid complex. A, Sequences of COMPcc and CSP with mutated arginine residue positions shown in red. B, Schematic of CSP complexation with plasmid DNA and a ternary complex with cationic lipids to form lipoproteoplexes for gene delivery. *In vitro* transfection efficiency for  $\beta$ -galactosidase DNA. FG\*DNA(4:1), COMPcc\*DNA(5:1), COMPcc\*DNA(5 or 8:1)\*FG, CSP\*DNA(5:1), CSP\*DNA(5 or 8:1)\*FG, mTat\*DNA(10:1) and mTat\*DNA(10:1)\*FG. C, comparison of control (DNA only), FG.DNA(4:1) etc., \* indicates  $P < 0.0001$ , D, comparison of control (DNA only), CSP\*DNA(8:1) etc., \* indicates  $P < 0.0001$ . Reproduced with permission<sup>[29]</sup>



#### 4.1 | Fusogenic peptide-polymer hybrids

Fusogenic peptides possess the ability to enhance the endosomal escape efficiency of polymeric gene delivery vectors. Gene delivery systems have been designed by conjugating cell-penetrating and membrane disruptive peptides with hydrophilic copolymers to promote effective intracellular delivery and endosomal escape.<sup>[31]</sup> For example, fluorescein-5-isothiocyanate (FITC) labeled N-(2-hydroxypropyl)methacrylamide (HPMA) copolymers, containing reactive ester groups and tert-butoxycarbonyl protected hydrazone bonds for post-polymer modification, can be synthesized by random polymerization. Multiple copies of octaarginine (R8) can then be decorated onto the HPMA copolymer (P-R8-FITC) to provide a local concentration of CPPs for effective intracellular delivery of siRNA into the cells.<sup>[31]</sup> A series of polymers have been synthesized with increasing R8 molar ratios (4-9.5 mol%) to determine the optimal R8 content for efficient oligonucleotide binding and cellular transduction. Gel retardation assay shows that among the polymers with variable content of cationic peptide tested, the polymer P-(R8)<sub>9.5</sub>-FITC with 9.5 mol% of R8 efficiently encapsulates RAC1 siRNA into polyion complexes. At <200 nm size, these complexes possess a positive charge of 18 mV at N/P ratio of 6. The P-(R8)<sub>9.5</sub>-FITC and Cy5-labeled-RAC1 siRNA complex further demonstrates successful internalization and accumulation in the cytoplasm of human ovarian adenocarcinoma cells (SK-OV-3). However, due to the weak membrane disrupting ability of R8, only a few siRNA molecules could escape the endosome, leading to low silencing of

RAC1 oncogene in cancer cells. To improve the gene silencing efficacy of polyplexes, the HA2 fusogenic peptide, derived from the N-terminal domain of the influenza virus hemagglutinin and recognized for the lysis of endosomal membranes, is attached to P-(R8)<sub>8.6</sub>-FITC. Conjugation of 7.4 mol% of membrane disrupting HA2 peptide to P-(R8)<sub>8.6</sub>-FITC (resulting in P-(R8)<sub>8.6</sub>-(HA2)<sub>7.6</sub>-FITC) demonstrates low cytotoxicity and significantly improved the RAC1 gene silencing in human lung carcinoma (A549 cells) (Figure 8). This indicates that grafting of R8 and HA2 peptides with HPMA copolymer leads to efficient delivery of the nucleic acids to the target cells and enhanced gene silencing.

In a study by Liu *et al.*, a 16-residue CPP called penetratin<sup>[96]</sup> derived from the DNA-binding domain of the *Drosophila* antennapedia homeoprotein is used to design a physical complex with a poly(amidoamine) (PAMAM) cationic dendrimer for intraocular gene delivery.<sup>[32]</sup> Three physical complexes comprising a penetratin-condensed red fluorescent protein plasmid (P20/pRFP), a PAMAM condensed pRFP (PAMAM/pRFP), and a penetratin-PAMAM double-condensed pRFP (pRFP/PAMAM/P20) have been synthesized to study the effect of the addition of penetratin and third generation non-cytotoxic vector PAMAM in condensation and delivery of nucleic acids. The preparation of the complexes involves simple mixing of the gene with the vectors. Synthesis of the pRFP/PAMAM/P20 complex comprises two steps: pRFP/PAMAM primary complex formation followed by addition of penetratin.

Particle size measurements of the complexes using TEM and DLS illustrate that the pRFP/P20 complex has the largest diameter

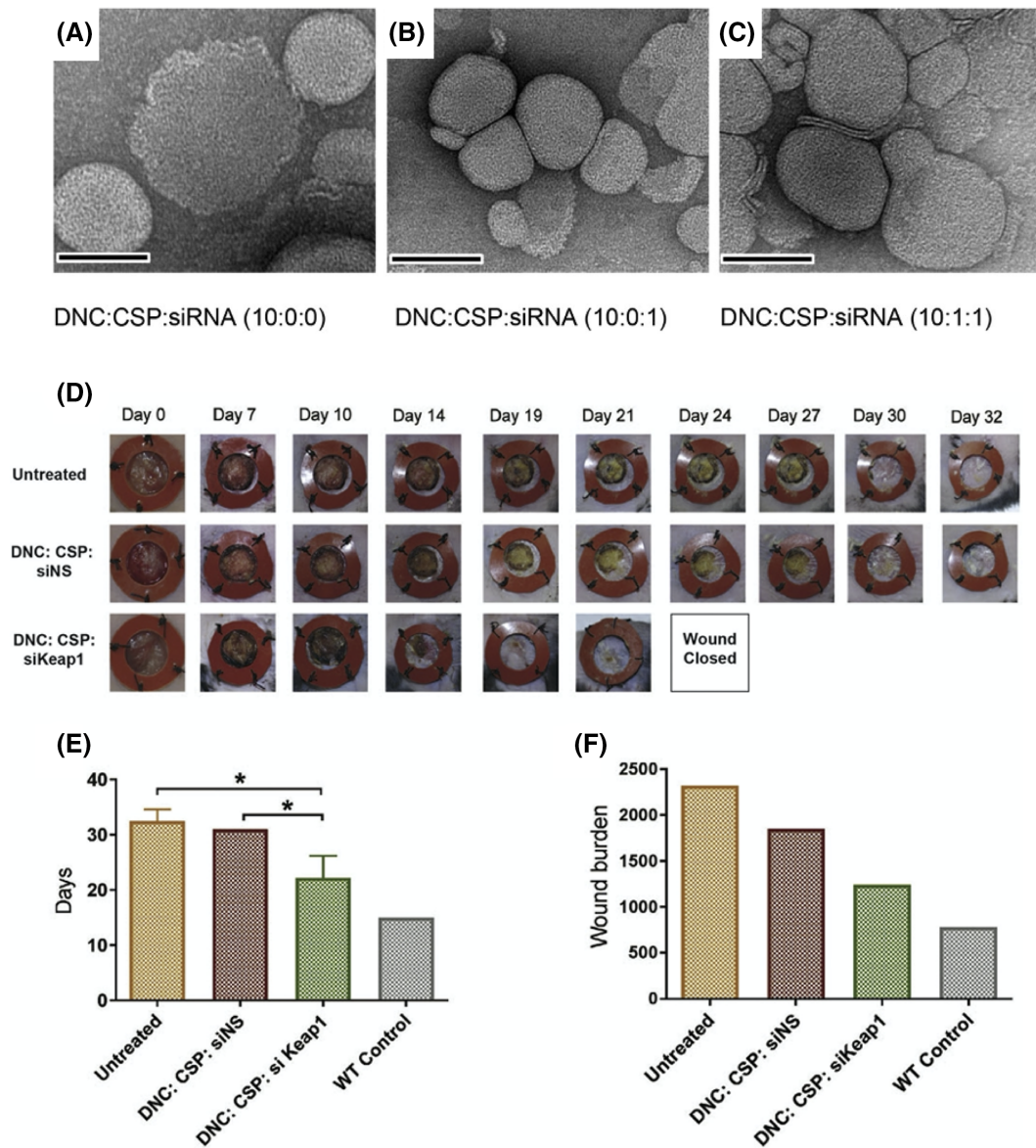


**FIGURE 7** DNC:CSP LPP for accelerated diabetic wound healing. TEM images of DNC:CSP:siRNA in the ratios, A, 10:0:0; B, 10:0:1; and C, 10:1:1. Scale bar, 100 nm. D, Images of stented wounds on diabetic mice with daily treatments as indicated; E, mean time to closure of wounds; and F, wound burden per treatment. Reproduced with permission<sup>[30]</sup>

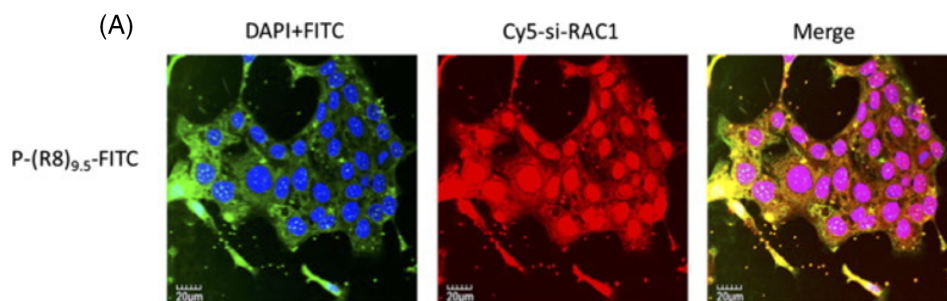
with a size of 420 nm, while pRFP/PAMAM particles are compact with a 260 nm size. The addition of penetratin further increases the condensation of the plasmid, with a reduction in particle size of pRFP/PAMAM/P20 complex to 150 nm. The tightly condensed nanoparticles of pRFP/PAMAM/P20 complex can be due to hydrophobic interactions between the tryptophan residues of penetratin and the internal cavities of PAMAM.<sup>[97]</sup> Stability of the complexes is tested by measuring the change in particles size over a period of 24 hours at eye temperature (34 °C). An increase in the particle size of pRFP/P20 and pRFP/PAMAM complexes is observed over time where pRFP/PAMAM/P20 complexes demonstrate highly stable particle size and lower tendency to aggregate because of its compact structure. Furthermore, owing to the

difference in particle size and internalization of the complexes, pRFP/PAMAM/P20 complex demonstrates high transfection efficiency in spontaneously derived human corneal epithelial cells as compared to pRFP/P20. *In vivo* examination of gene expression is performed by installing the complexes in the conjunctival sac in the eyes of rats. Topical application of pRFP alone does not transfect the retina, however both pRFP/P20 and pRFP/PAMAM/P20 can penetrate from the ocular surface into the fundus. The pRFP/PAMAM/P20 complex induces more efficient gene expression of RFP in the posterior segment than pRFP/P20 as observed from the fluorescence images of the retina (Figure 9). This study demonstrates a novel approach towards noninvasive intraocular gene delivery.

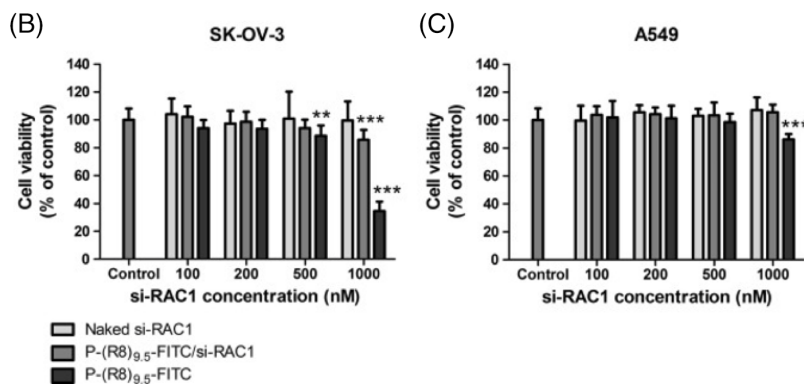
## 4.2 | Stimuli-responsive peptide-polymer hybrids

A number of peptides and polymers have the ability to degrade themselves in response to external stimuli and can be incorporated into polyplexes to allow the facile display of membrane lytic moieties to promote endosomal escape.<sup>[33,98]</sup> Cheng *et al.* have designed VIPER (virus-inspired polymer for endosomal release), a self-assembling polymer to mimic the endosomal escape mechanism of adenovirus.<sup>[33]</sup> VIPER is comprised of two blocks: a hydrophilic cationic block to condense nucleic acids and a pH-sensitive block that allows conformational modification under acidic conditions to display melittin, a membrane-lytic peptide for triggering endo/lysosomal escape. Melittin has the ability to make channels in the lipid membrane,<sup>[99]</sup> and has been used to complex with various polymer-based gene delivery vectors to promote endosomal escape.<sup>[100]</sup> Reversible addition-fragmentation chain transfer (RAFT) polymerization was employed to synthesize the copolymer (denoted as CP) comprised of poly(oligo

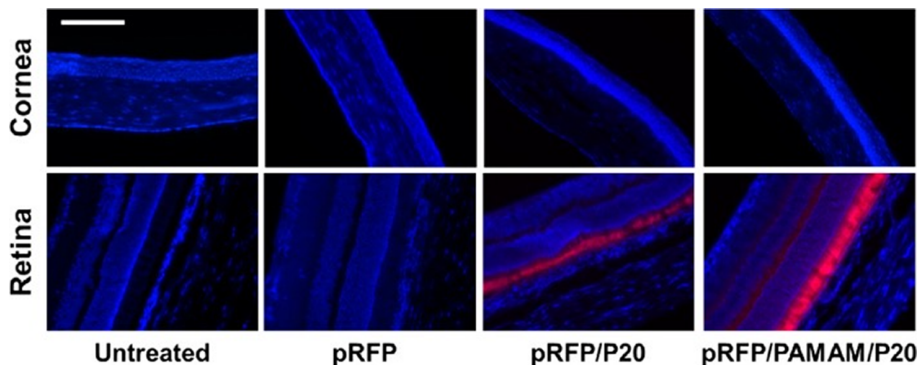
(ethylene glycol) monomethyl ether methacrylate)-co-poly(2-(dimethylamino)ethyl methacrylate) (p(OEGMA-DMAEMA)) as the hydrophilic block and poly(2-diisopropylaminoethyl methacrylate)-co-poly(pyridyl disulfide ethyl methacrylate) (p(DIPAMA-PDSEMA)) as the pH responsive block. CP is conjugated with cysteine-melittin through a disulfide exchange reaction to form VIPER that self-assembles into micelles at physiological pH with melittin in the hydrophobic core. The pH-triggered phase transition of VIPER is assessed by analyzing its assembly at pH 7.4 and 5.7. Formation of nanoparticles with 30 nm diameter is observed at pH 7.4 whereas no such assembly is witnessed at endosomal pH (pH 5.7), indicating the dissociation of particles. Both CP and VIPER demonstrates the ability to effectively condense plasmid DNA to form compact spherical nanoparticles with diameters less than 100 nm. The efficiency of endosomal escape of nucleic acid cargo from VIPER and CP polyplexes is evaluated in HeLa cells using confocal microscopy. The results indicate significantly enhanced endosomal release in the case of the VIPER polyplex compared



**FIGURE 8** R8 and HA2 grafted HPMA based polyplexes. A, Confocal images of SK-OV-3 cells transfected with P-(R8)<sub>9,5</sub>-FITC/Cy5-labeled siRNA (red), green—FITC, blue—DAPI. B, *In vitro* cytotoxicity of P-(R8)<sub>8,6</sub>-(HA2)<sub>7,6</sub>-FITC/RAC1 siRNA against A549 cells. C, Transfection of A549 cells with RAC1 siRNA complexed with P-(R8)<sub>8,6</sub>-(HA2)<sub>7,6</sub>-FITC. Reproduced with permission<sup>[31]</sup>



**FIGURE 9** Penetratin-PAMAM mediated intraocular gene delivery. Fluorescence images of corneas and retinas of rat bulbus oculi illustrating RFP expression after topical administration of pRFP plasmid alone and the complexes. Blue, DAPI-labeled cell nuclei; red, expressed RFP. Scale bar = 50  $\mu$ m. Reprinted with permission.<sup>[32]</sup> Copyright © 2016, American Chemical Society



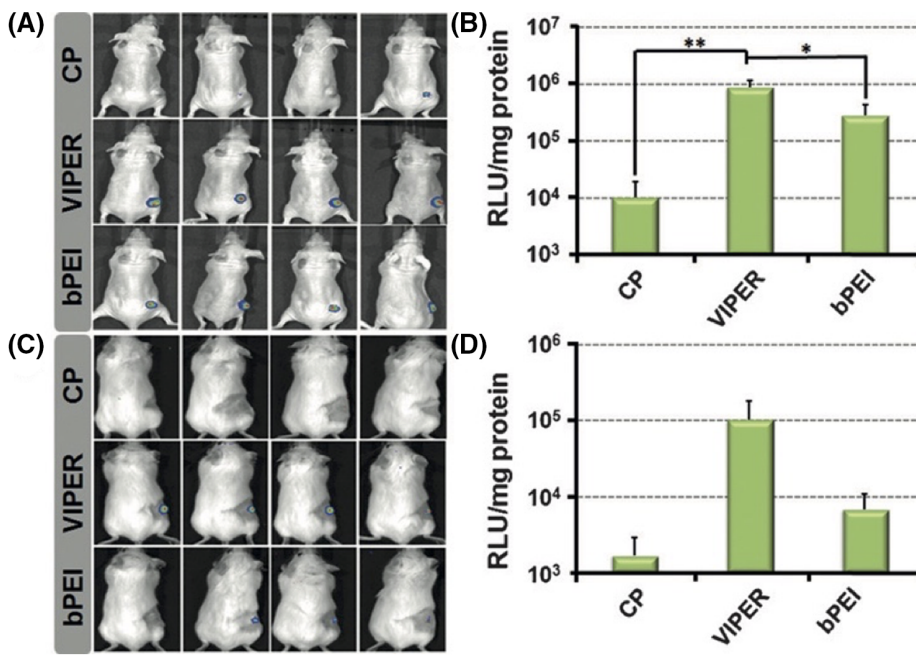


**FIGURE 10** pH-responsive peptide-polymer hybrid. A, Bioluminescence images of KB-tumor-bearing mice treated with various polyplexes. B, Luciferase activity from excised KB tumor tissues of mice treated with polyplexes. C, Bioluminescence images of A549-tumor-bearing mice treated with various polyplexes. D, Luciferase activity from excised A549 tumor tissues of mice treated with polyplexes. Data are shown as mean  $\pm$  SD (n = 4; Student's *t* test, \**P* < .05, \*\**P* < .01). Reprinted with permission<sup>[33]</sup>

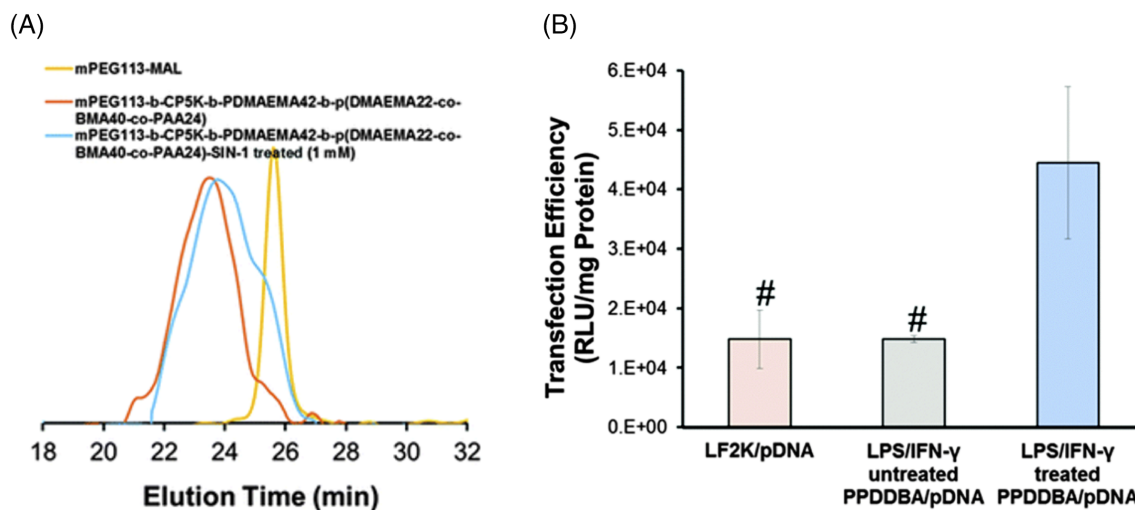


**FIGURE 11** ROS cleavable pH-responsive polyplexes. A, GPC chromatograms of PPDDBP with the appearance of shoulder peak of PPDDBP (blue) overlapping the PEG peak (yellow) indicating ROS-mediated detachment of PEG block from PPDDBP polymer through cleavage of CP5K peptide after treatment with SIN-1. B, Transfection efficiency of PPDDBP polyplexes with and without LPS/IFN- $\gamma$  treatment and LF2K containing luciferase pDNA assessed in HCASMCs. Reproduced with permission<sup>[34]</sup>

to CP. To further evaluate VIPER's capability as a gene delivery vector, KB and A549 xenograft tumor models are employed. KB tumors treated with VIPER polyplexes containing a luciferase plasmid show enhanced gene transfer efficacy with 3.1- and 82.5-fold higher luciferase activity compared to branched PEI and CP polyplexes, respectively (Figure 10A, B). Similar results are observed in A549 xenograft tumors with 15.1-fold and 59.7-fold higher activity in VIPER polyplex treated tumors than PEI and CP polyplexes, respectively (Figure 10C, D). The collective results signify the potential of VIPER for pH responsive gene-delivery.

Reactive oxygen species (ROS), an excessive production of hydrogen peroxide, are a common occurrence in vascular smooth muscle cells (VSMCs) at critical stages of atherosclerosis.<sup>[101]</sup> Efforts have been made to design gene-delivery vectors that allows facile release of nucleic acids in

response to ROS species present in the pathological microenvironment.<sup>[102–104]</sup> Gupta *et al.* have designed a pH and ROS-responsive polyplex as a gene delivery platform for targeting the pathological vascular microenvironment.<sup>[34]</sup> The multifunctional peptide-polymer hybrid is synthesized by conjugating ROS cleavable cysteine-(proline)<sub>5</sub>-lysine (CP<sub>5</sub>K) peptide with PEG to form a macrochain transfer agent that is further used for RAFT polymerization to form ROS-cleavable, pH-responsive cationic copolymers made of mPEG-b-CP<sub>5</sub>K-b-poly dimethyl aminoethyl methacrylamide-b-[poly (dimethylaminoethyl methacrylamide)-co-poly(butyl methacrylate)-co-poly(acrylic acid)] (termed as PPDDBP). ROS-triggered dePEGylation of PPDDBP micelles is confirmed by overnight incubation with peroxyntirite producing 3-morpholinosydnonimine (SIN-1).

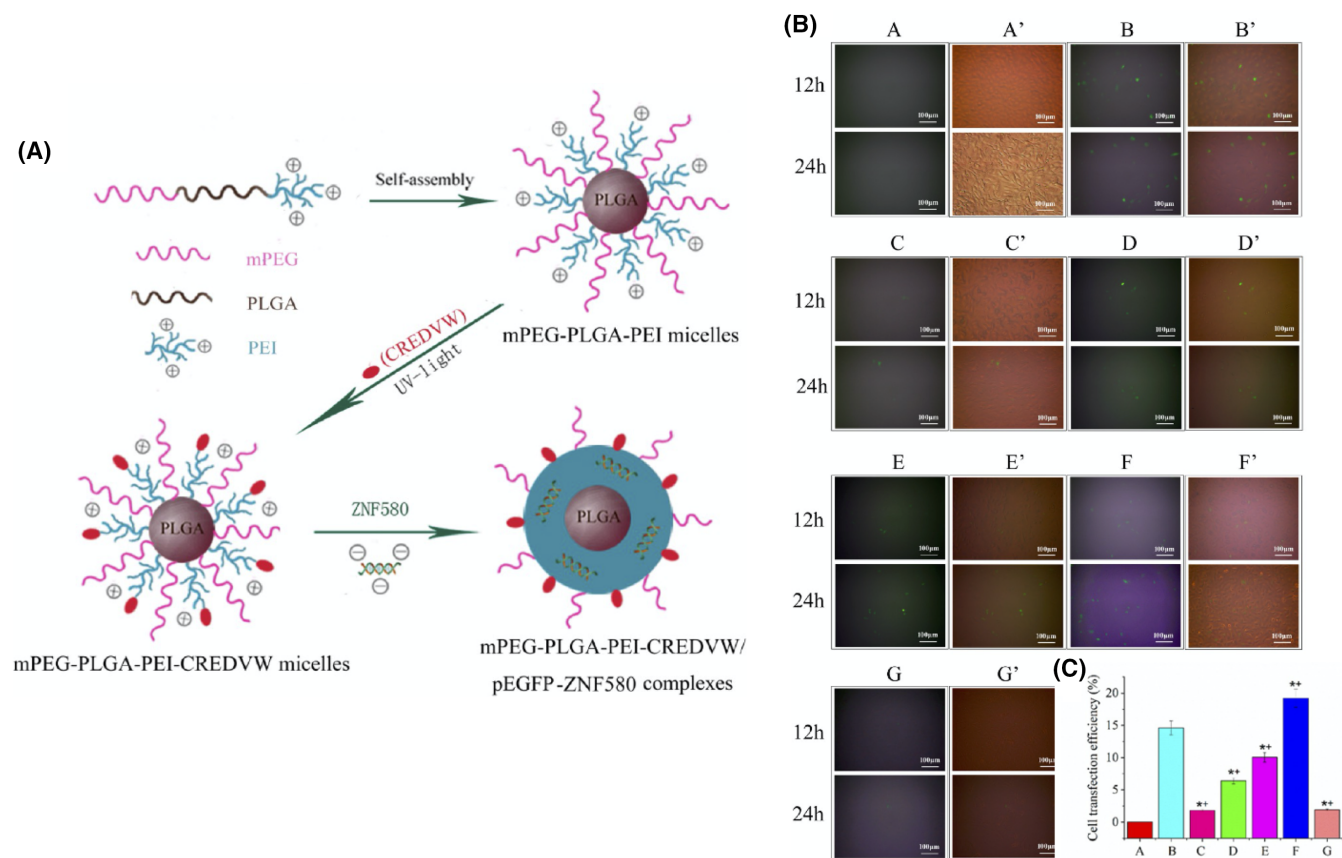


**FIGURE 12** REDV conjugated polymer micelles for targeted gene delivery. A, Self-Assembly of mPEG-b-PLGA-g-PEI-CREDVW micelles and the formation of mPEG-b-PLGA-g-PEI-CREDVW/pEGFP-ZNF580 complexes. B, Fluorescence images of EA.hy926 cells and rat vascular SMCs (as a control) transfected with the complexes with the N/P molar ratio of 20 at time intervals of 12 and 24 hr and C, the transfection efficiency at 24 h. A, EA.hy926 cells treated with pDNA served as the negative control; B, EA.hy926 cells treated with Lipofectamine 2000/pDNA served as positive control group; C, EA.hy926 cells treated with mPEG-b-PLGA-g-PEI(1.8 kDa)-REDV/pDNA complexes; D, EA.hy926 cells treated with mPEG-b-PLGA-g-PEI(1.8 kDa)-REDV/pDNA complexes; E, EA.hy926 cells treated with mPEG-b-PLGA-g-PEI(10 kDa)-REDV/pDNA complexes; F, EA.hy926 cells treated with mPEG-b-PLGA-g-PEI(10 kDa)-REDV/pDNA complexes; G, rat vascular SMCs treated with mPEG-b-PLGA-g-PEI(10 kDa)-REDV/pDNA complexes. (A', B', C', D', E', F', and G' are the bright-field images, and A, B, C, D, E, F, and G are the corresponding dark-field images, respectively) ( $\bar{x} \pm SD$ ,  $n = 3$ , \*statistically different from cells treated with pDNA group ( $P < .05$ ), \*\*statistically different from cells treated with Lipofectamine 2000/pDNA group ( $P < .05$ )). Reprinted with permission.<sup>[35]</sup> Copyright © 2015, American Chemical Society

Reduction in molecular weight of the polymer and appearance of a PEG shoulder in gel permeation chromatography indicates successful dePEGylation due to cleavage of CP<sub>2</sub>K peptide (Figure 11).

Transfection efficiency of PPDDBP/luciferase pDNA polyplexes with and without lipopolysaccharide and interferon gamma (LPS/IFN- $\gamma$ ) treatment is also assessed in human coronary artery smooth muscle cells (HCASMCs). The results indicate high transfection efficiency of LPS/IFN- $\gamma$  treated PPDDBP polyplexes that is ~2.5-fold higher than that of untreated HCASMCs and commercially available lipofectamine2000 (LF2K) polyplexes. These results suggest the applicability of these multifunctional polyplexes as a carrier for gene delivery.

### 4.3 | Targeting peptide-polymer hybrids

The incorporation of specific peptides into gene transfer vectors allows the delivery of nucleic acid to the desired location *in vivo*.<sup>[105]</sup>

One of the most widely used recognition site for targeting endothelial cells is the Arg-Gly-Asp (RGD) peptide.<sup>[106,107]</sup> However, RGD suffers from poor selectivity towards endothelial cells. Arg-Glu-Asp-Val (REDV), a short peptide derived from fibronectin can selectively bind to endothelial cells due to its recognition sites for integrin  $\alpha 4\beta 1$  binding.<sup>[108,109]</sup> Hao *et al.* have investigated a REDV conjugated self-assembling polymer micelle with high targeting efficacy to endothelial cells.<sup>[35]</sup> Polyethylenimine (PEI) is a well-studied polymeric gene transfer vector with high transfection efficiency owing to the proton-sponge effect.<sup>[110,111]</sup> PEI with high molecular weights have been demonstrated to exhibit high transfection efficacy and cytotoxicity.<sup>[112]</sup> In this study, low-molecular-weight branched PEI having acceptable cytotoxicity but lower transfection ability is explored by generating micelles with of two self-assembling block copolymers comprised of a biodegradable poly(lactide-co-glycolide) (PLGA) core and a mixed methoxy-poly(ethylene glycol) (mPEG)/PEI (1.8 or 10 kDa) shell (Figure 12A). In order to endow the mPEG-b-PLGA-g-

PEI micelles with targeting ability, a CREVDW peptide containing the REDV sequence is covalently attached to the micelles by a thiol–ene click-reaction to provide targeting ability by increasing endothelial cell recognition. A non-targeting control is designed by conjugating inactive REVD to the micelles for studying the specific targeting of REDV polyplexes.

The polymeric micelles with and without the peptide demonstrate efficient condensation of pEGFP-ZNF580 plasmid to form complexes with a diameter less than 150 nm. REDV peptide targeted polyplexes exhibits very high transfection efficacy and gene expression in human endothelial cell lines (EA.hy926 cells) when compared to the control REVD-modified polyplexes, emphasizing the selective targeting of REDV polyplexes for endothelial cells (Figure 12B,C). The low cytotoxicity and high transfection efficiency of REDV-conjugated micelles indicate its potential applicability as a gene delivery vector for endothelialization of artificial blood vessels.

## 5 | CONCLUSIONS AND FUTURE OUTLOOK

CPPs and oligopeptides are versatile materials that can be used to deliver nucleic acids using a variety of mechanisms. They are able to condense and protect nucleic acids on their own or can be combined with other types of materials, such as lipids and polymers, to impart new function and enhance delivery properties. The inclusion of new functional components to peptide sequences is particularly interesting as it allows for multi-functional materials that improve gene delivery by several parallel mechanisms. CPPs and oligopeptide-based systems have been shown to be as or more effective than lipid-based and polymer-based reagents for *in vitro* and *in vivo* transfection, and combining peptides with these systems allows for development of new designs that leverage the benefits of multiple material types at once. Up until now, a majority of work has been validated in cell culture systems,<sup>[19,21,35,113]</sup> but more work needs to be done to assess peptide-based materials in animal systems. Peptides alone can be susceptible to a variety of nucleases and harsh environmental conditions, so combining them with other materials may be crucial as development goes forward. This may produce problems with the toxicity of the other materials, such as polymers and cationic lipids, so a balance must be struck between delivery efficiency and cytotoxicity. The use of amino acid building blocks presents almost endless permutations of sequence however, so it is likely that new CPP sequences will be identified and refined as time goes on which will add to the already existing toolbox. Non-canonical amino acids have been used to optimize peptide and protein materials for other applications outside of gene delivery,<sup>[114,115]</sup> such as the use of analogs of phenylalanine to improve the pharmacological properties of the antibiotic peptide nisin<sup>[116]</sup> and the use of *p*-fluorophenylalanine to improve the thermostability of a phosphotriesterase enzyme.<sup>[117]</sup> A photo-caged lysine variant has also been incorporated into an adenovirus vector at a site responsible for host cell entry that allows for temporal control of viral infection via a 365 nm light stimulus.<sup>[118]</sup> Non-canonical amino acids

may therefore be introduced into CPP or oligopeptide sequences to optimize chemical properties and further improve/control transfection. Overall, peptides are an excellent alternative to viral based vectors and may very soon surpass them in both efficacy and safety. Peptides provide the ability to condense nucleic acids, but also possess the ability to cross the cell membrane and even escape the endosome, making them powerful components when used in non-viral delivery vectors. As non-viral vectors continue moving closer and closer to widespread clinical use, all of the promises of nucleic acid therapies may finally be realized.

## ACKNOWLEDGEMENTS

This work was supported by NSF-DMREF under Award Number DMR 1728858, NSF BMAT under Award Number DMR 1505214, ARO W911NF-19-1-0150 and W911NF-19-2-0160, the NYU Shiffrin-Myers Breast Cancer Discovery Fund, and the NYU CTSA grant UL1 TR000038 from the National Center for Advancing Translational Sciences, National Institutes of Health.

## CONFLICT OF INTEREST

The authors declare no competing interests.

## DATA AVAILABILITY STATEMENT

Data sharing is not applicable to this article as no new data were created or analyzed in this study.

## ORCID

Jin Kim Montclare  <https://orcid.org/0000-0001-6857-3591>

## REFERENCES

- [1] F. Wang, Z. Qin, H. Lu, S. He, J. Luo, C. Jin, X. Song, *J. Gen. Med.* **2019**, 21, e3108.
- [2] Y. H. Chen, M. S. Keiser, B. L. Davidson, *Curr. Protoc. Mouse. Biol.* **2018**, 8, e58.
- [3] H. Lv, S. Zhang, B. Wang, S. Cui, J. Yan, *J. Controlled Release* **2006**, 114, 100.
- [4] R. Goswami, G. Subramanian, L. Silayeva, I. Newkirk, D. Doctor, K. Chawla, S. Chattopadhyay, D. Chandra, N. Chilukuri, V. Betapudi, *Front. Oncol.* **2019**, 9, 297.
- [5] A. K. Varkouhi, M. Scholte, G. Storm, H. J. Haisma, *J. Controlled Release* **2011**, 151, 220.
- [6] C. Barnes, O. Scheideler, D. Schaffer, *Curr. Opin. Biotechnol.* **2019**, 60, 99.
- [7] S. C. De Smedt, J. Demeester, W. E. Hennink, *Pharm. Res.* **2000**, 17, 113.
- [8] S. M. G. Hayat, N. Farahani, E. Safdarian, A. Roointan, A. Sahebkar, *Crit. Rev. Eukaryot. Gene Expr.* **2019**, 29, 29.
- [9] M. Dorrani, O. B. Garbuzenko, T. Minko, B. Michniak-Kohn, *J. Controlled Release* **2016**, 228, 150.
- [10] N. Khatri, D. Baradia, I. Vhora, M. Rathi, A. Misra, *AAPS PharmSciTech* **2014**, 15, 1630.
- [11] A. Kwok, D. McCarthy, S. L. Hart, A. D. Tagalakis, *Chem. Biol. Drug Des.* **2016**, 87, 747.
- [12] Y. Wan, P. M. Moyle, M. P. Christie, I. Toth, *Nanomedicine (London)* **2016**, 11, 907.
- [13] Y. Lei, L. Tang, Y. Xie, Y. Xianyu, L. Zhang, P. Wang, Y. Hamada, K. Jiang, W. Zheng, X. Jiang, *Nat. Commun.* **2017**, 8, 15130.
- [14] M. K. Riley, W. Vermerris, *Nanomaterials (Basel)* **2017**, 7, 94.

- [15] R. Shi, W. Lian, S. Han, C. Cao, Y. Jin, Y. Yuan, H. Zhao, M. Li, *Gene Ther.* **2018**, *25*, 425.
- [16] J. P. Campbell, T. J. McFarland, J. T. Stout, *Dev. Ophthalmol.* **2016**, *55*, 317.
- [17] A. Oryan, E. Alemzadeh, M. Zarei, *Biotechnol. Lett.* **2019**, *41*, 889.
- [18] J. Woo, S. H. Bae, B. Kim, J. S. Park, S. Jung, M. Lee, Y. H. Kim, D. Choi, *PLoS One* **2015**, *10*, e0144491.
- [19] J. Yoo, D. Lee, V. Gujrati, N. S. Rejinold, K. M. Lekshmi, S. Uthaman, C. Jeong, I. K. Park, S. Jon, Y. C. Kim, *J. Controlled Release* **2017**, *246*, 142.
- [20] H. Mandal, S. S. Katiyar, R. Swami, V. Kushwah, P. B. Katore, A. Kumar Meka, S. K. Banerjee, A. Popat, S. Jain, *Int. J. Pharm.* **2018**, *542*, 142.
- [21] D. P. Walsh, R. D. Murphy, A. Panarella, R. M. Raftery, B. Cavanagh, J. C. Simpson, F. J. O'Brien, A. Heise, S. A. Cryan, *Mol. Pharmaceutics* **2018**, *15*, 1878.
- [22] X. Quan, D. Sun, J. Zhou, *Phys. Chem. Chem. Phys.* **2019**, *21*, 10300.
- [23] S. Yamano, C. T. Viet, D. Dang, J. Dai, S. Hanatani, T. Takayama, H. Kasai, K. Imamura, R. Campbell, Y. Ye, J. C. Dolan, W. M. Kwon, S. D. Schneider, B. L. Schmidt, *Pain* **2017**, *158*, 240.
- [24] C. Jeong, J. Yoo, D. Lee, Y. C. Kim, *Biomater. Res.* **2016**, *20*, 28.
- [25] H. Song, B. Oh, M. Choi, J. Oh, M. Lee, *J. Drug Targeting* **2015**, *23*, 360.
- [26] X. Liang, B. Shi, K. Wang, M. Fan, D. Jiao, J. Ao, N. Song, C. Wang, J. Gu, Z. Li, *Biomaterials* **2016**, *82*, 194.
- [27] E. H. Ervin, M. Pook, I. Teino, V. Kasuk, A. Trei, M. Pooga, T. Maimets, *Stem Cell Res. Ther.* **2019**, *10*, 43.
- [28] E. Urgard, A. Brjalín, Ü. Langel, M. Pooga, A. Rebane, T. Annilo, *Nucleic Acid Ther.* **2017**, *27*, 295.
- [29] H. T. More, J. A. Frezzo, J. Dai, S. Yamano, J. K. Montclare, *Biomaterials* **2014**, *35*, 7188.
- [30] P. S. Rabbani, A. Zhou, Z. M. Borab, J. A. Frezzo, N. Srivastava, H. T. More, W. J. Rifkin, J. A. David, S. J. Berens, R. Chen, S. Hameedi, M. H. Junejo, C. Kim, R. A. Sartor, C. F. Liu, P. B. Saadeh, J. K. Montclare, D. J. Ceradini, *Biomaterials* **2017**, *132*, 1.
- [31] M. Golan, V. Feinshtein, A. David, *Eur. J. Pharm. Biopharm.* **2016**, *109*, 103.
- [32] C. Liu, K. Jiang, L. Tai, Y. Liu, G. Wei, W. Lu, W. Pan, *ACS Appl. Mater. Interfaces* **2016**, *8*, 19256.
- [33] Y. Cheng, R. C. Yumul, S. H. Pun, *Angew. Chem. Int. Ed.* **2016**, *55*, 12013.
- [34] M. K. Gupta, S. H. Lee, S. W. Crowder, X. Wang, L. H. Hofmeister, C. E. Nelson, L. M. Bellan, C. L. Duvall, H.-J. Sung, *J. Mater. Chem. B* **2015**, *3*, 7271.
- [35] X. Hao, Q. Li, J. Lv, L. Yu, X. Ren, L. Zhang, Y. Feng, W. Zhang, *ACS Appl. Mater. Interfaces* **2015**, *7*, 12128.
- [36] G. Y. Wu, C. H. Wu, *Biochemistry* **1988**, *27*, 887.
- [37] D. M. Copolovici, K. Langel, E. Eriste, Ü. Langel, *ACS Nano* **2014**, *8*, 1972.
- [38] A. Pensado, F. J. Diaz-Corrales, B. De la Cerda, L. Valdés-Sánchez, A. A. Del Boz, D. Rodriguez-Martinez, A. B. García-Delgado, B. Seijo, S. S. Bhattacharya, A. Sanchez, *Nanomedicine* **2016**, *12*, 2251.
- [39] L. Tai, C. Liu, K. Jiang, X. Chen, G. Wei, W. Lu, W. Pan, *Nanomedicine* **2017**, *13*, 2091.
- [40] X. Cai, C. Dong, H. Dong, G. Wang, G. M. Pualetti, X. Pan, H. Wen, I. Mehl, Y. Li, D. Shi, *Biomacromolecules* **2012**, *13*, 1024.
- [41] H. Kuang, S. H. Ku, E. Kokkoli, *Adv. Drug Delivery Rev.* **2017**, *110–111*, 80.
- [42] A. Parthasarathy, S. K. Anandamma, K. A. Kalesh, *Curr. Med. Chem.* **2019**, *26*, 2330.
- [43] R. E. Taylor, M. Zahid, *Pharmaceutics* **2020**, *12*, 225.
- [44] J. S. Liou, B. R. Liu, A. L. Martin, Y. W. Huang, H. J. Chiang, H. J. Lee, *Peptides* **2012**, *37*, 273.
- [45] S. Yamano, J. Dai, C. Yuvienco, S. Khapli, A. M. Moursi, J. K. Montclare, *J. Controlled Release* **2011**, *152*, 278.
- [46] C. W. Pouton, P. Lucas, B. J. Thomas, A. N. Uduehi, D. A. Milroy, S. H. Moss, *J. Controlled Release* **1998**, *53*, 289.
- [47] I. Ruseska, A. Zimmer, *Beilstein J. Nanotechnol.* **2020**, *11*, 101.
- [48] E. Alinejad-Mofrad, B. Malaekheh-Nikouei, L. Gholami, S. H. Mousavi, H. R. Sadeghnia, M. Mohajeri, M. Darroudi, R. K. Oskuee, *Hum. Exp. Toxicol.* **2019**, *38*, 983.
- [49] O. Veisesh, F. M. Kievit, V. Liu, C. Fang, Z. R. Stephen, R. G. Ellenbogen, M. Zhang, *Mol. Pharmaceutics* **2013**, *10*, 4099.
- [50] J. S. Wadia, S. F. Dowdy, *Curr. Opin. Biotechnol.* **2002**, *13*, 52.
- [51] Y. W. Won, H. A. Kim, M. Lee, Y. H. Kim, *Mol. Ther.* **2010**, *18*, 734.
- [52] H. Hyun, Y. W. Won, K. M. Kim, J. Lee, M. Lee, Y. H. Kim, *Biomaterials* **2010**, *31*, 9128.
- [53] Y. W. Won, K. M. Kim, S. S. An, M. Lee, Y. Ha, Y. H. Kim, *Biomaterials* **2011**, *32*, 9766.
- [54] Z. Taimeh, J. Loughran, E. J. Birks, R. Bolli, *Nat. Rev. Cardiol.* **2013**, *10*, 519.
- [55] D. Oupický, A. L. Parker, L. W. Seymour, *J. Am. Chem. Soc.* **2002**, *124*, 8.
- [56] D. J. Phillips, M. I. Gibson, *Biomacromolecules* **2012**, *13*, 3200.
- [57] N. J. Baumhover, J. T. Duskey, S. Khargharia, C. W. White, S. T. Crowley, R. J. Allen, K. G. Rice, *Mol. Pharmaceutics* **2015**, *12*, 4321.
- [58] P. Saccardo, A. Villaverde, N. González-Montalbán, *Biotechnol. Adv.* **2009**, *27*, 432.
- [59] A. Dodd, D. Swanevelder, N. Zhou, D. Brady, J. E. Hallsworth, K. Rumbold, *J. Ind. Microbiol. Biotechnol.* **2018**, *45*, 1083.
- [60] G. A. Eggimann, E. Blattes, S. Buschor, R. Biswas, S. M. Kammer, T. Darbre, J. L. Reymond, *Chem. Commun.* **2014**, *50*, 7254.
- [61] X. Cai, Y. Li, D. Yue, Q. Yi, S. Li, D. Shi, Z. Gu, *J. Mater. Chem. B* **2015**, *3*, 1507.
- [62] A. Erazo-Oliveras, N. Muthukrishnan, R. Baker, T. Y. Wang, J. P. Pellois, *Pharmaceuticals (Basel)* **2012**, *5*, 1177.
- [63] L. Hyndman, J. L. Lemoine, L. Huang, D. J. Porteous, A. C. Boyd, X. Nan, *J. Controlled Release* **2004**, *99*, 435.
- [64] A. Macho, M. A. Calzado, L. Jiménez-Reina, E. Ceballos, J. León, E. Muñoz, *Oncogene* **1999**, *18*, 7543.
- [65] X. Chen, J. Chen, R. Fu, P. Rao, R. Weller, J. Bradshaw, S. Liu, *J. Pharm. Sci.* **2018**, *107*, 879.
- [66] E. K. Bang, H. Cho, S. S. Jeon, N. L. Tran, D. K. Lim, W. Hur, T. Sim, *Chem. Biol. Drug Des.* **2018**, *91*, 575.
- [67] L. A. Avila, L. R. M. M. Aps, N. Ploscariu, P. Sukthankar, R. Guo, K. E. Wilkinson, P. Games, R. Szoszkiewicz, R. P. S. Alves, M. O. Diniz, Y. Fang, L. C. S. Ferreira, J. M. Tomich, *J. Controlled Release* **2016**, *241*, 15.
- [68] J. A. Chan, A. M. Krichevsky, K. S. Kosik, *Cancer Res.* **2005**, *65*, 6029.
- [69] T. Papagiannakopoulos, A. Shapiro, K. S. Kosik, *Cancer Res.* **2008**, *68*, 8164.
- [70] J. Lee, H. Hyun, J. Kim, J. H. Ryu, H. A. Kim, J. H. Park, M. Lee, *J. Controlled Release* **2012**, *158*, 131.
- [71] J. H. Park, H. A. Kim, M. Lee, *Biomaterials* **2012**, *33*, 6542.
- [72] O. Boussif, F. Lezoualc'h, M. A. Zanta, M. D. Mergny, D. Scherman, B. Demeneix, J. P. Behr, *Proc. Natl. Acad. Sci. U. S. A.* **1995**, *92*, 7297.
- [73] M. Thomas, K. Lange-Grünweller, E. Dayyoub, U. Bakowsky, U. Weirauch, A. Aigner, R. K. Hartmann, A. Grünweller, *RNA Biol.* **2012**, *9*, 1088.
- [74] A. Malek, O. Merkel, L. Fink, F. Czubyayko, T. Kissel, A. Aigner, *Toxicol. Appl. Pharmacol.* **2009**, *236*, 97.
- [75] H. Jiang, Q. Dong, X. Luo, B. Shi, H. Wang, H. Gao, J. Kong, J. Zhang, Z. Li, *Cancer Lett.* **2014**, *342*, 113.
- [76] P. Zhang, B. Shi, H. Gao, H. Jiang, J. Kong, J. Yan, X. Pan, K. Li, M. Yao, S. Yang, J. Gu, H. Wang, Z. Li, *Cancer Immunol. Immunother.* **2014**, *63*, 121.
- [77] M. Zhou, H. Wang, K. Zhou, X. Luo, X. Pan, B. Shi, H. Jiang, J. Zhang, K. Li, H. M. Wang, H. Gao, S. Lu, M. Yao, Y. Mao, H. Y. Wang, S. Yang, J. Gu, C. Li, Z. Li, *Cancer Res.* **2013**, *73*, 7056.
- [78] P. Arukuusk, L. Pärnaste, M. Hällbrink, Ü. Langel, *Methods Mol. Biol.* **2015**, *1324*, 303.

- [79] J. Suhorutsenko, N. Oskolkov, P. Arukuusk, K. Kurrikoff, E. Eriste, D. M. Copolovici, U. Langel, *Bioconjugate Chem.* **2011**, *22*, 2255.
- [80] K. Ezzat, S. E. Andaloussi, E. M. Zaghoul, T. Lehto, S. Lindberg, P. M. Moreno, J. R. Viola, T. Magdy, R. Abdo, P. Guterstam, R. Sillard, S. M. Hammond, M. J. Wood, A. A. Arzumanov, M. J. Gait, C. I. Smith, M. Hällbrink, Ü. Langel, *Nucleic Acids Res.* **2011**, *39*, 5284.
- [81] H. Hermeking, *Cell Death Differ.* **2010**, *17*, 193.
- [82] H. Wang, F. Wang, X. Wang, X. Wu, F. Xu, K. Wang, M. Xiao, X. Jin, *Med. Sci. Monit.* **2019**, *25*, 1952.
- [83] C. Liu, K. Kelnar, B. Liu, X. Chen, T. Calhoun-Davis, H. Li, L. Patrawala, H. Yan, C. Jeter, S. Honorio, J. F. Wiggins, A. G. Bader, R. Fagin, D. Brown, D. G. Tang, *Nat. Med.* **2011**, *17*, 211.
- [84] J. F. Wiggins, L. Ruffino, K. Kelnar, M. Omotola, L. Patrawala, D. Brown, A. G. Bader, *Cancer Res.* **2010**, *70*, 5923.
- [85] S. Al-Taei, N. A. Penning, J. C. Simpson, S. Futaki, T. Takeuchi, I. Nakase, A. T. Jones, *Bioconjugate Chem.* **2006**, *17*, 90.
- [86] S. B. Fonseca, M. P. Pereira, S. O. Kelley, *Adv. Drug Delivery Rev.* **2009**, *61*, 953.
- [87] I. S. Zuhorn, J. B. F. N. Engberts, D. Hoekstra, *Eur. Biophys. J.* **2007**, *36*, 349.
- [88] R. G. Jenkins, S. E. Herrick, Q. H. Meng, C. Kinnon, G. J. Laurent, R. J. McNulty, S. L. Hart, *Gene Ther.* **2000**, *7*, 393.
- [89] F. Zhou, X. Jia, Q. Yang, Y. Yang, Y. Zhao, Y. Fan, X. Yuan, *Biomater. Sci.* **2016**, *4*, 849.
- [90] J. W. Salameh, L. Zhou, S. M. Ward, C. F. Santa Chalarca, T. Emrick, M. L. Figueiredo, *WIREs Nanomed. Nanobiotechnol.* **2020**, *12*, e1598.
- [91] M. Ahmed, *Biomater. Sci.* **2017**, *5*, 2188.
- [92] A. C. Eldredge, M. E. Johnson, N. J. Oldenhuis, Z. Guan, *Biomacromolecules* **2016**, *17*, 3138.
- [93] J. Lv, X. Hao, Q. Li, M. Akpanyung, A. Nejjari, A. L. Neve, X. Ren, Y. Feng, C. Shi, W. Zhang, *Biomater. Sci.* **2017**, *5*, 511.
- [94] M. Byrne, D. Victory, A. Hibbitts, M. Lanigan, A. Heise, S.-A. Cryan, *Biomater. Sci.* **2013**, *1*, 1223.
- [95] J. Shi, R. N. Johnson, J. G. Schellinger, P. M. Carlson, S. H. Pun, *Int. J. Pharm.* **2012**, *427*, 113.
- [96] D. Derossi, A. H. Joliot, G. Chassaing, A. Prochiantz, *J. Biol. Chem.* **1994**, *269*, 10444.
- [97] P. E. S. Smith, J. R. Brender, U. H. N. Dürr, J. Xu, D. G. Mullen, M. M. Banaszak Holl, A. Ramamoorthy, *J. Am. Chem. Soc.* **2010**, *132*, 8087.
- [98] D. Soundara Manickam, H. S. Bisht, L. Wan, G. Mao, D. Oupicky, *J. Controlled Release* **2005**, *102*, 293.
- [99] M. T. Tosteson, D. C. Tosteson, *Biophys. J.* **1981**, *36*, 109.
- [100] M. Ogris, R. C. Carlisle, T. Bettinger, L. W. Seymour, *J. Biol. Chem.* **2001**, *276*, 47550.
- [101] C. H. Byon, J. M. Heath, Y. Chen, *Redox Biol.* **2016**, *9*, 244.
- [102] K. Han, Q. Lei, H.-Z. Jia, S.-B. Wang, W.-N. Yin, W.-H. Chen, S.-X. Cheng, X.-Z. Zhang, *Adv. Funct. Mater.* **2015**, *25*, 1248.
- [103] M. S. Shim, Y. Xia, *Angew. Chem. Int. Ed.* **2013**, *52*, 6926.
- [104] Y. Yuan, C.-J. Zhang, B. Liu, *Angew. Chem. Int. Ed.* **2015**, *54*, 11419.
- [105] T. O. Pangburn, M. A. Petersen, B. Waybrant, M. M. Adil, E. Kokkoli, *J. Biomech. Eng.* **2009**, *131*, 074005.
- [106] R. Liu, X. Chen, S. H. Gellman, K. S. Masters, *J. Am. Chem. Soc.* **2013**, *135*, 16296.
- [107] Y. Liu, T. T. Yang Tan, S. Yuan, C. Choong, *J. Mater. Chem. B* **2013**, *1*, 157.
- [108] Y. Wei, Y. Ji, L.-L. Xiao, Q.-k. Lin, J.-p. Xu, K.-f. Ren, J. Ji, *Biomaterials* **2013**, *34*, 2588.
- [109] Y. Wei, Y. Ji, L. Xiao, Q. Lin, J. Ji, *Colloids Surf., B* **2011**, *84*, 369.
- [110] D. R. Holycross, M. Chai, *Macromolecules* **2013**, *46*, 6891.
- [111] R. Kircheis, L. Wightman, A. Schreiber, B. Robitzka, V. Rössler, M. Kurska, E. Wagner, *Gene Ther.* **2001**, *8*, 28.
- [112] M. Bartneck, K.-H. Heffels, Y. Pan, M. Bovi, G. Zwadlo-Klarwasser, J. Groll, *Biomaterials* **2012**, *33*, 4136.
- [113] J. H. Kang, G. Battogtokh, Y. T. Ko, *Biomacromolecules* **2017**, *18*, 3733.
- [114] A. R. Nödling, L. A. Spear, T. L. Williams, L. Y. P. Luk, Y. H. Tsai, *Essays Biochem.* **2019**, *63*, 237.
- [115] Y. Huang, T. Liu, *Synth. Syst. Biotechnol.* **2018**, *3*, 150.
- [116] C. Zambaldo, X. Luo, A. P. Mehta, P. G. Schultz, *J. Am. Chem. Soc.* **2017**, *139*, 11646.
- [117] C. Y. Yang, P. D. Renfrew, A. J. Olsen, M. Zhang, C. Yuvienco, R. Bonneau, J. K. Montclare, *ChemBioChem* **2014**, *15*, 1761.
- [118] S. B. Erickson, R. Mukherjee, R. E. Kelemen, C. J. Wrobel, X. Cao, A. Chatterjee, *Angew. Chem. Int. Ed. Engl.* **2017**, *56*, 4234.

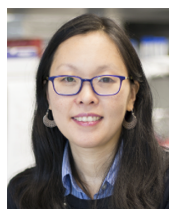
## AUTHOR BIOGRAPHIES



**JOSEPH THOMAS** is currently a Ph.D. candidate studying biomedical engineering in a joint program with New York University (NYU) Tandon School of Engineering and the State University of New York (SUNY) Downstate (USA). His work focuses on the development of protein and lipid vectors for gene delivery. He previously earned both a B.S. and M.S from Kent State University (USA) studying biochemistry and biophysics, specifically focusing on lipid membrane dynamics.



**KAMIA PUNIA** obtained her Ph.D. in chemistry from The Graduate Center of the City University of New York (USA) focusing on the synthesis and characterization of macromolecules for biomedical applications. She is a postdoctoral fellow in Prof. Jin Kim Montclare's lab at NYU Tandon School of Engineering (USA). Her research is focused on engineered coiled-coil protein biomaterials for theranostic applications.



**JIN KIM MONTCLARE** is a Professor in the Chemical and Biomolecular Engineering Department at NYU Tandon School of Engineering (USA) and Director of the Convergence for Innovation and Entrepreneurship Institute with appointments in Chemistry at NYU, Biomaterials at NYU College of Dentistry and Radiology at NYU School of Medicine. She exploits nature's biosynthetic machinery and evolutionary mechanisms to design new artificial proteins. Among her many honors are the AAAS Leshner Fellow (2019), AIMBE Fellow (2019), and ACS WCC Rising Star Award (2016).

**How to cite this article:** Thomas J, Punia K, Montclare JK. Peptides as key components in the design of non-viral vectors for gene delivery. *Peptide Science*. 2021;113:e24189. <https://doi.org/10.1002/pep2.24189>